RHODIUM(0) NANOPARTICLES SUPPORTED ON TITANIUM DIOXIDE: SYNTHESIS AND CHARACTERIZATION FOR HYDROGEN GENERATION FROM THE HYDROLYSIS OF AMMONIA BORANE

by

SERAP GENÇTÜRK

THESIS SUBMITTED TO

THE GRADUATE SCHOOL OF NATURAL AND APPLIED SCIENCES

OF

THE ABANT İZZET BAYSAL UNIVERSITY

IN PARTIAL FULFILLMENT OF THE REQUIREMENTS FOR THE DEGREE OF

MASTER OF SCIENCE

IN

DEPARTMENT OF CHEMISTRY

JUNE 2014

Approval of the Graduate School of Natural and Applied Sciences

Prof. Dr. Yaşar DÜRÜST
Director

I certify that this thesis satisfies all the requirements as a thesis for the degree of Master of Science.

Prof. Dr. Nedime DÜRÜST
Head of the Department

This is to certify that we have read this thesis and that in our opinion it is fully adequate, in scope and quality, as a thesis for the degree of Master of Science.

Prof. Dr. Saim ÖZKÂR
Co-advisor

Prof. Dr. İzzet MORKAN
Supervisor

Examining Committee Members

1- Prof. Dr. İzzet MORKAN
2- Prof. Dr. Nusret ZENCİRCİ
3- Assist. Prof. Dr. Erhan BUDAK

ABSTRACT

RHODIUM(0) NANOPARTICLES SUPPORTED ON TITANIUM DIOXIDE: SYNTHESIS AND CHARACTERIZATION FOR HYDROGEN GENERATION FROM THE HYDROLYSIS OF AMMONIA BORANE

Gençtürk, Serap

M.Sc., Department of Chemistry

Supervisor: Prof. Dr. İzzet Amour MORKAN

JUNE 2014, 62 Pages

The activity of catalyst is directly related to its surface area, the reduction of particle size of the catalyst is a promising way to increase the catalytic activity. An efficient way of increasing catalytic activity is the usage of metal nanoclusters which are expected to be more active catalysts than the respective bulk metal counterparts, because a large percentage of atoms are on the surface of nanoclusters. This dissertation reports the preparation, characterization and investigation of the catalytic activity of rhodium(0) nanoparticles supported on the surface of titanium dioxide ($Rh(0)@TiO_2$) were in situ generated from the reduction of rhodium(III) ions impregnated on nanotitania during the hydrolysis of ammonia borane. They were isolated from the reaction solution by centrifugation and characterized by a combination of advanced analytical techniques as ICP-OES, XRD, SEM-EDS, TEM,

XPS and the N_2 adsorption-desorption spectroscopy. Highly dispersed rhodium(0) nanoparticles of size in the range 1.3-3.8 nm were formed on the surface of titanium dioxide. Kinetics of the hydrogen generation from the hydrolysis of ammonia borane in the presence of rhodium(0) nanoclusters were investigated depending on catalyst concentration, substrate concentration and temperature. As a result, hydrogen generation rate was found to be first-order with respect to the catalyst concentration and zero-order regarding the substrate concentration. In addition rhodium(0) nanoparticles supported on nanotitania show high catalytic activity in hydrogen generation from the hydrolysis of ammonia borane with a turnover frequency value up to 260 min^{-1} at room temperature. Moreover, the results of kinetic study on the hydrogen generation from the hydrolysis of ammonia borane were also reported including the activation energy of 65.5 ± 2 kJ/mol for this reaction.

Keywords: Rhodium(0) nanoparticles, Titanium dioxide, Hydrolysis of ammonia borane, Hydrogen generation.

ÖZET

TİTANYUM DİOKSİT ÜZERİNDE TUTTURULMUŞ RODYUM(0) NANOPARÇACIKLARI: AMONYAK BORANIN HİDROLİZİNDEN HİDROJEN ÜRETİMİ İÇİN SENTEZİ VE KARAKTERİZASYONU

GENÇTÜRK, SERAP

Yüksek Lisans, Kimya Bölümü

Tez Yöneticisi: Prof. Dr. İzzet Amour MORKAN

HAZİRAN 2014, 62 Sayfa

Katalizörün aktivitesi direkt onun yüzey alanıyla ilgili olup, katalizörün aktivitesini artırmak için parçacık boyutunun küçültülmesi umut veren bir yöntemdir. Katalitik aktiviteyi artırmanın etkili yollarından biri, kendi metal külçe benzerlerinden daha aktif katalizör olan metal nanokümeleri kullanmaktır. Bunun nedeni; atomların büyük yüzdesinin nanokümelerin yüzeyinde olmasındandır. Bu tezde amonyak boranın hidrolizi sırasında nanotitanyaya emdirilmiş olan rodyum(III) iyonlarının indirgenmesinden oluşan titanyum dioksitin yüzeyinde tutturulan rodyum(0) nanoparçacıklarının hazırlanışı, karakterizasyonu ve katalitik aktivitesi araştırıldı. Rodyum(0) nanoparçacıklar reaksiyon çözeltisinden santrifüj ile izole edilip, ICP-OES, XRD, SEM-EDS, TEM, XPS ve N_2 yüzey tutunma-salınma spektroskopisi gibi ileri analitik teknikleri kullanılarak karakterize edildi. Titanyum

dioksit yüzeyinde oluşturulan yüksek dağılımlı rodyum(0) nanoparçacıklarının boyutu 1.3-3.8 nm aralığındadır. Rodyum(0) nanokümelerinin varlığında amonyak boranın hidrolizinden hidrojen üretiminin kinetiği; katalizör derişimine, tepken derişimine ve sıcaklığa bağlı olarak çalışıldı. Tepkime derecesinin, katalizör derişimine göre birinci, tepken derişimine göre sıfırıncı dereceden olduğu saptandı. Ek olarak, nanotitanya üzerinde desteklendirilmiş rodyum(0) nanoparçacıkları oda sıcaklığında 260 dk^{-1} çevrim frekansı değeriyle amonyak boranın hidrolizinden hidrojen üretiminde yüksek katalitik aktivite gösterdi. Ayrıca, kinetik çalışmanın sonuçlarına göre bu reaksiyon için aktivasyon enerjisi 65.5 ± 2 kJ/mol aralığında bulunmuştur.

Anahtar Kelimeler: Rodyum(0) nanoparçacıklar, Titanyum dioksit, Amonyak boranın hidrolizi, Hidrojen üretimi.

To my family;

ACKNOWLEDGEMENTS

I would like to express my greatest gratitude to my advisor, Prof. Dr. İzzet MORKAN for his great support, encouragement, quidance and understanding throughout in this study.

I wish to say my sincere appreciations to my co-advisor, Prof. Dr. Saim ÖZKÂR for his concern and valuable advices. He provided facility of working in Chemistry Department of Middle East Technical University. I am lucky to have a chance to work with him.

I would like also thank to Prof. Dr. Ayşe UZTETİK MORKAN for her motivation, valuable advices and moral support.

I want to give my special thanks to Serdar AKBAYRAK who is a member of Middle East Technical University for his supports, patience, advices, motivation and helping me with every problem I encountered during my studies.

I especially thank to Seda TANYILDIZI for her frendship, moral support, helping and discussions during completion of the thesis.

The last but not the least, I would like to extend my gratitude to my father, Mustafa Kadri Gençtürk, and my mother, Türkan Gençtürk for their endless support, endless patience and helping me with every problem I encountered in every step of my life.

TABLE OF CONTENT

LIST OF FIGURES

LIST OF TABLE

LIST OF ABBREVATIONS

ICP-OES : Inductively Coupled Plasma - Optical Emission spectroscopy

TEM : Transmission Electron Microscopy

SEM : Scanning Electron Microscopy

XRD : X - Ray Diffraction

XPS : X - Ray Photoelectron Spectroscopy

Uv-vis : Ultraviolet Visible Spectroscopy

NPs : Nanoparticles

AB : Ammonia borane

Rh^{3+}@TiO_2 : Rh^{3+}-Exchanged titanium dioxide

Rh(0)@TiO_2 : Rhodim(0) Nanoparticles Supported on Titanium dioxide

TOF : Turnover Frequency

TON : Turnover Number

Ea : Activation Energy

INTRODUCTION

The global energy demand is increasing with increase in population, modernization, and industrialization. To meet its energy requirements, the world at present relies heavily on fossil fuels such as coal, oil, and gas. However, the world's natural resources are depleting rapidly leading to a pandemic energy crisis [1]. Furthermore, the excessive use of carbon-based fuels is adding tremendous amount of green house gases in the atmosphere and raising the temperature of the planet at an alarmingly rapid rate [2,3]. Therefore, it is important to search for nonpolluting and renewable sources of energy to replace fosil fuels and to satisfy the energy need of the growing global population.

During the past several decades, there have been considerable researchs and developments in the areas of the environmentally friendly fuels and energy technology [4,5]. Hydrogen has emerged as one of the strongest candidates for the following reasons:

- Hydrogen exhibits the highest heating value per mass of all chemical fuels. The energy content of hydrogen (142 MJ/kg) is nearly three times that of liquid hydrocarbons (47 MJ/kg) [6].
- Hydrogen is non - toxic and when it is oxidized water is the only exhaust product. Therefore, hydrogen is an extremely clean fuel.
- Hydrogen is the ideal candidate for the fuel cells. The energy conversion efficiency of hydrogen fuel cells is not limited by the efficiency of Carnot cycles and

can theoretically reach 100%, which is multiple times the efficiency of internal combustion engines [7,8].

- Hydrogen can be produced from water by using renewable sources of energy.

Thus, it is widely believed that hydrogen can help to address the increasing demand for energy and retard global climate change. Therefore, it reduces dependency on foreign oil [9].

Hydrogen is the most abundant element in the universe. It is estimated that the universe is made up of 92% hydrogen, 7 % helium and 1% consist of other elements [10]. Hydrogen is the tenth most abundant element in the earth's crust and can be found everywhere on the surface of the earth as a component of water. It is found in fossil fuels, all plants and animals (e.g. carbohydrates and proteins), ammonia, acids, and a variety of other compounds. However, hydrogen is unavailable in elemental form in earth's atmosphere due to its reactive nature. Hydrogen must be extracted from, for example, water or organic compounds by using some primary energy sources, such as fossil fuels, solar, nuclear, or wind. Therefore, hydrogen is not a source of energy but a synthetic energy carrier [6].

Once produced, hydrogen has to be stored, distributed and converted into energy. The widespread production, storage, distribution, and use of hydrogen as an energy carrier is called the hydrogen economy [11]. Regardless of its application, hydrogen storage is a very challenging technical and economic issue to be overcome before the hydrogen economy can be realized on global scale [12]. Hydrogen can be stored physically by changing its state conditions (compressed gas or cryogenic liquid) and chemically in various solid compounds such as metal nitrides and imides [13], carbon nanotubes [14], TiO_2 nanotubes [15], zeolites [16], organic polymers [17], metal-organic frameworks [18] and carbon-boron-nitrogen (CBN) compounds

[19]. Among these materials, borone nitrogen containing compounds such as sodium borohydride, ammonia borane, hydrazine-borane methylamine borane and dimethylamine borane have attracted much attention due to their low weight and high gravimetric capacity [20]. Furthermore, the results of recent studies have presented that ammonia-borane (NH_3BH_3, AB) has been regarded as one of the leading candidates as hydrogen storage materials for on-board hydrogen applications due to its high hydrogen storage capacity (19.6 wt %), nontoxicity and high stability under ambient conditions [21]. AB is solid at room ambient temperatures due to it is strongly polar molecule and having strong intermolecular interactions based on different electronegativities of B and N atoms. AB is nontoxic, stable at ambient temperatures, environmentally harmless, readily available and can be handled at room temperature. It is thermally stable enough to transport and store. Also, it is stable in air and aqueous solutions and in absence of catalysts or protic solvents there is no liberation of hydrogen observed. AB can release hydrogen via thermolysis [22], hydrolysis [23], and methanolysis [24]. Since the high temperature is required for the former, [25] the hydrolysis reaction is highly advantageous for the hydrogen generation from AB. However, hydrogen stored in AB can be released at appreciable rate via hydrolysis only in the presence of a suitable catalyst (eq.1) [26,27]. Therefore, the development of efficient and stable catalysts under moderate conditions is vital for the practical applications.

$$H_3NBH_3(aq) + 2H_2O(l) \xrightarrow{catalyst} NH_4^+(aq) + BO_2^-(aq) + 3H_2(g) \quad (1)$$

A number of catalysts have been tested in hydrogen generation from the hydrolysis of AB, including transition metal nanoparticles such as platinum, rhodium, ruthenium, palladium, cobalt and nickel [28,29]. Although rhodium, platinum and ruthenium metal nanoparticles have high price and limited abundance,

they are superior to the non-noble metal nanoparticles due to their long life-time and high activity in the hydrolysis of ammonia borane. Therefore the use of noble metal nanoparticles as catalysts has been intensively studied in recent years. Metal nanoparticles exhibit much higher catalytic activity compared to the bulk metal due to the large fraction of atoms on their surface. However, metal nanoparticles tend to aggregate into clumps causing a decrease in catalytic activity [30,31]. Titanium dioxide with large surface area ranging from 10 to 300 m^2/g, can be used as a support to prevent the aggregation of metal nanoparticles. Titanium dioxide is one of the suitable catalysts for environmental applications because of its nontoxicity, strong oxidizing power and the high stability against corrosion [32]. Titanium dioxide has also been extensively studied as a semiconductor material due to its wide band gap and low cost [33].

The aim of this study is the preparation, characterization of rhodium(0) nanoparticles supported on titania (Rh(0)@TiO_2) and their employment in the hydrogen generation from the hydrolysis of ammonia-borane. Herein we report the *in situ* generation, characterization, and catalytic use of rhodium(0) nanoparticles supported on titanium dioxide with particle size of about 100 nm, hereafter referred to as Rh(0)@TiO_2. Rhodium(III) ions impregnated on the surface of titania particles was reduced by ammonia borane forming the Rh(0)@TiO_2 without using any additional reducing agent during the hydrolysis of ammonia borane. The use of *in situ* generation of Rh(0)@TiO_2 provides the opportunity to avoid the laborious catalyst preparation steps. Rh(0)@TiO_2 were isolated from the reaction solution and characterized by ICP-OES, XRD, TEM, SEM-EDS, XPS and the N_2 adsorption–desorption techniques. The hydrolysis of ammonia borane catalyzed by rhodium(0) nanoparticles was followed by monitoring the volume of hydrogen generation versus

time. Kinetics of catalytic hydrolysis of AB was studied depending on the catalyst concentration, substrate concentration, and temperature. The activity of rhodium(0) nanoparticles supported on titania was maintained after the redispersion of the sample isolated from the solution after complete hydrolysis of ammonia-borane. The evolution of 3 equivalents of hydrogen from the hydrolysis of ammonia-borane confirms the activity of preformed catalyst.

CHAPTER 2

2. HYDROGEN ECONOMY

2.1. Global Energy Problems

Energy is an essential and ubiquitous part of our daily lives, it is a basic material of human survival and development. In the international social, political and economic environment, any development of economic globalization, social modernization and national industrialization is inseparable from a strong energy security. As more and more fosil fuels are used, energy has been increasing its impact on the environment and restricting the development of human economy and society [34].

Global energy consumption is expected to increase dramatically in the next decades, driven by rising standards of living and a growing population worldwide. The increased need for more energy will require enormous growth in energy generation capacity, more secure and diversified energy sources, and a successful strategy to tame greenhouse gas emissions. Among the various alternative energy strategies, building an energy infrastructure that uses hydrogen (the third most abundant element on the earth's surface) as the primary carrier that connects a host of energy sources to diverse end uses may enable a secure and clean energy future for the nation.

It is clear that assuring the security of the energy supply for the U.S. over the next few decades will present major problems. There are a number of reasons for this; the most important of these is the current reliance on fosil fuels for a high proportion of the energy, of which a significant fraction is imported. The Developing World countries will have greatly increased needs for energy, in part because of the expected population increase, and in part because of the increase in their presently very low standards of living. A second problem is related to concerns over the environmental effects of the use of fosil fuels. Third, the peaking of the production of fosil fuels is likely within the next several decades [35].

The world of 21st century will be challenged by the need to expand the energy supply and reduce greenhouse gas emissions. At present, the global population is more than 6.5 billion, and estimated to reach 10 billion in the mid-21 century. Therefore, only from the perspective increase in population, the growth in global energy demand will be enormous. As the major energy sources of current structure, fossil fuel resources are finite, just as the forest will become wilderness if there is only cutting and no planting, so large amount of energy use will soon deplete these non-renewable energy resources. In addition, the large volume of emission from energy industry, especially fosil fuel has made global environmental problems severe [36].

All these make world energy problems more complex and more difficult to solve, how to develop and utilize world energy in 21 century is not a future issues, but an urgent event that concerns humans' destiny. The important thing people need to consider is how to cognize energy status, study energy supply and demand structure patterns from different perspectives, analyze the driving forces and constrains of energy development, discuss how energy industry impact on economy

development and global environment, conclude energy development trends and seek its changes rules, so as to adopt relevant strategies and measurements to achieve a sustainable E3 System (Energy-Economy-Environment).

2.2. Hydrogen as an Energy Carrier

Hydrogen is an abundant element on Earth (Schlapbach & Züttel, 2001) and primarily occurs as a component of other substances, for example, water and hydrocarbons such as oil and coal, but rarely on its own as H_2 (U.S. DOE, 2008b). Therefore, it is necessary to invest energy to free the element from the compound, and thus, hydrogen is an energy carrier, like electricity, rather than an energy source (U.S. DOE, 2008b). Hydrogen is first isolated in 1766 by Henry Cavendish. Fuel-cell developments have been started by the year 1839 and it is stil studying by researchers [37].

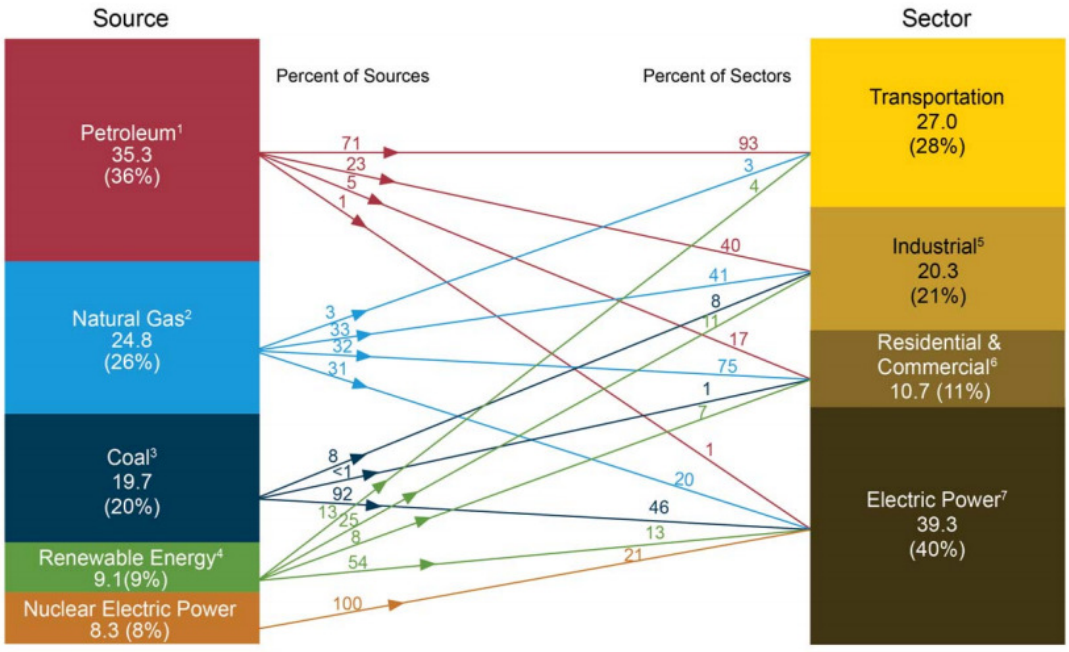

Figure 2.2.1. Primary Energy Consumption by Source and Sector [38]

Energy sources are used mainly for transportation sector, in industrial applications, residential and commercial usage and finally for electric power. U.S Energy Information Administration (EIA) reported primary energy consumption by source and sector (Figure 2.2.1.) [38].

More than 67% of this energy was consumed for electric and transportation purposes, as shown in Figure 2.2.1. Most of this energy came from non-renewable sources, (i.e., petroleum, natural gas, and coal) representing more than 80% of the total supply sources. These issues motivates interest to replace current energy-related technologies with cleaner ones that support sustainable global economic growth including reduction of the impacts on air quality and potential effects of greenhouse gas emissions for the near, mid and long term future [39].

One of the solutions proposed is the use of hydrogen (H_2) as an energy carrier. Hydrogen is considered the 'forever fuel', since, like electricity, its secondary energy 'running mate,' it can be produced from any primary energy fuel: coal, oil, natural gas, nuclear, all sorts of renewable energies, and from grid electricity [40]. But the use of hydrogen as the world's dominant energy carrier is limited by a series of technological, infrastructural, and political hurdles. Hydrogen gas is expensive to produce, and current methods of production rely heavily on fossil fuels such as steam methane reforming [41]. Hydrogen gas is difficult to store economically; compressed gas has very low density and requires significant volume, and liquid hydrogen storage requires cryogenic capabilities resulting in evaporative losses of about one third of the total hydrogen being stored [42]. Hydrogen delivery technologies cost more than conventional fuel Technologies and dispensing systems are expensive [43].

The importance of hydrogen as a potential energy carrier has increased significantly over the last decade, owing to rapid advances in fuel cell technology. Fuel cells, operating using hydrogen or hydrogen-rich fuels, have the potential to become major factors in catalysing the transition to a future sustainable energy system with low carbon dioxide emissions. The importance of such developments is rapidly increasing; many countries are now compiling roadmaps, in many cases with specific numerical targets for the advancement of fuel cell and hydrogen technologies.

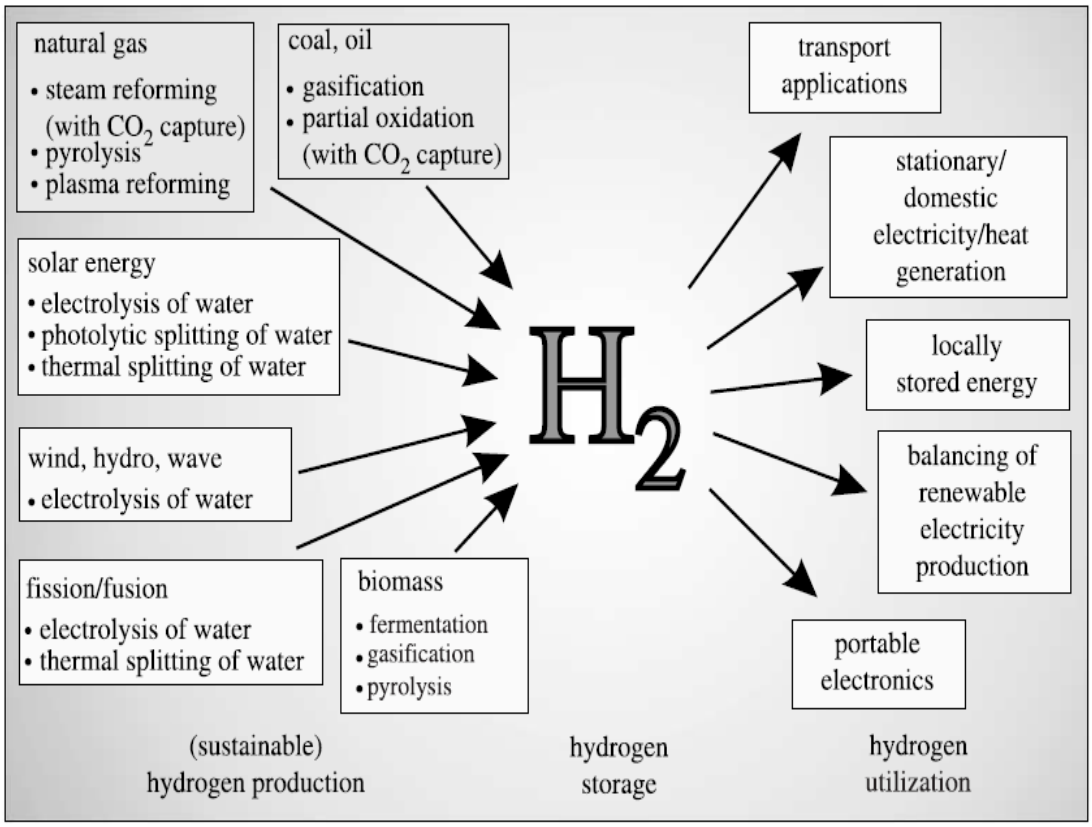

Figure 2.2.2. Hydrogen as an energy carrier linking multiple hydrogen production methods, through storage to various end-users. Shaded production routes can involve substantial carbon dioxide (by-product) generation.

Figure 2.2.2. illustrates the central role of hydrogen as an energy carrier linking multiple hydrogen production methods and various end-user applications.

One of the principal attractions of hydrogen as an energy carrier is obviously the diversity of production methods from a variety of resources. Hydrogen can be produced from coal, natural gas and other hydrocarbons by a variety of techniques, from water by electrolysis, photolytic splitting or high-temperature thermochemical cycles, from biomass and even municipal waste. Such a diversity of production sources contributes significantly to the security of energy supply.

Hydrogen can be stored in different forms, each presenting specific advantages and disadvantages. Energy density, volume, efficiency, and safety are the main factors to be considered in contemplating hydrogen storage [44]. The methods via which hydrogen can be stored are: as a compressed gas, as a liquid, or chemically combined into a metal hydride. Underground storage is still another option for hydrogen storage, even though it is just a special case of compressed gas. Hydrogen storage will be needed to meet the time-varying demand for fuel [45] similarly to today's needs for natural gas and gasoline storage.

Hydrogen is expected to be the fuel in the near future. At present hydrogen fuel is mainly produced using steam reforming of methane (SRM). However, hydrogen generation using the SRM results in emission of greenhouse gases and climate change. Therefore, there is a common consensus that the SRM technology will soon be challenged by the technologies of solar hydrogen generation using photoelectrochemical cells (PEC). However, the PEC technology will be the ultimate winner only if the effects related to climate change and pollution are fully monetised. While such radical development is difficult for implementation due to economic reasons, the increasingly urgent need to reduce climate change dictates the need to increase competitiveness of the PEC method. This imposes the need to increase the

efficiency of the solar energy conversion and reduce the costs of the related raw materials and devices [46].

2.3. Ammonia-Borane as a Hydrogen Storage Material

One of the major obstacles to the widespread use of hydrogen as an energy carrier, especially for transportation applications, is the lack of safe and efficient means for hydrogen storage. Decades of extensive efforts on metal/alloy hydrides, nanostructured carbon materials, and complex hydrides have not led to a viable system that can reversibly store over 6wt % hydrogen at a moderate temperature range [47–50]. Recently, irreversible hydrogen storage via catalyzed hydrolysis or thermolysis of chemical/metal hydrides has emerged as an alternative and more promising solution for on-board hydrogen storage [51,52]. Among the hydride materials of interest, ammonia borane (NH_3BH_3, AB) is a leading candidate, which is justified by its extremely high gravimetric hydrogen capacity (19.6 wt %) shown in figure 2.3.1. and relatively favorable thermal stability.

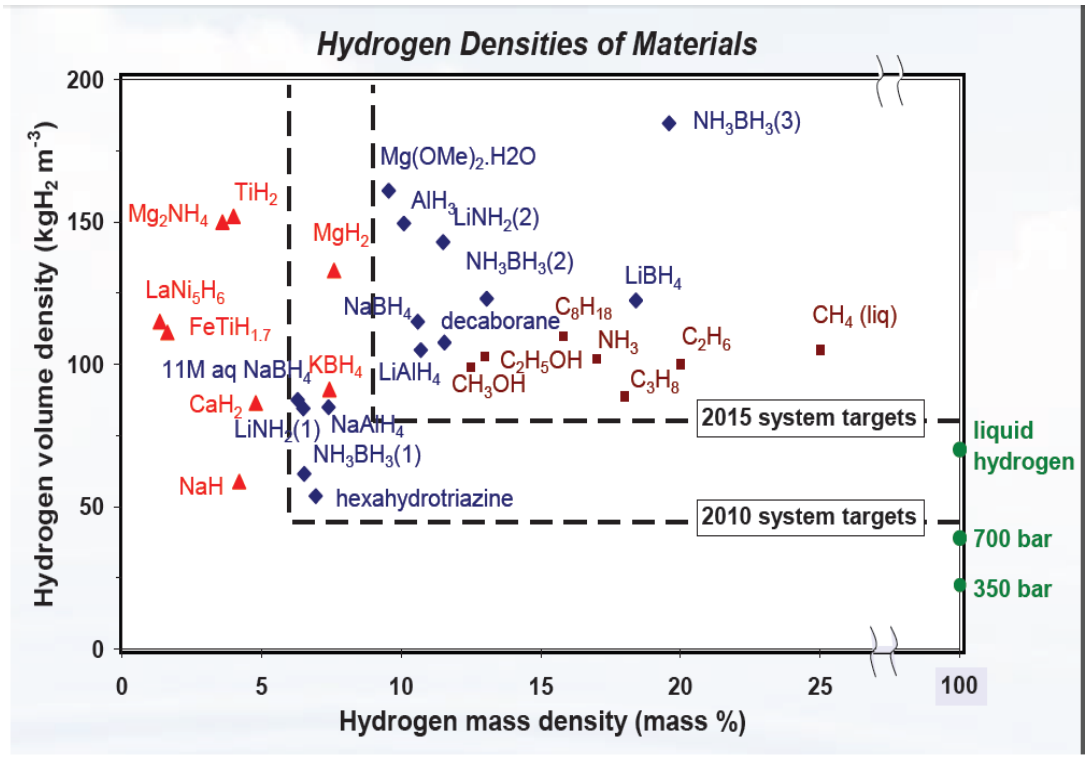

Figure 2.3.1. Volumetric hydrogen density versus gravimetric hydrogen density of various hydrogen containing compounds (adopted from the literature [53]).

AB composed of B and N atoms which creates a big electronegativity difference and contains both hydridic B–H and protonic N–H bonds within the same molecule. This fact results in strong molecular attractions between atoms, so AB is solid at room temperature which enables extra stability to AB at ambient temperatures. Moreover it is nontoxic and environmentally benign. AB can release hydrogen via catalyzed hydrolysis in an aqueous solution, [23,54] catalyzed dehydrocoupling under non-aqueous conditions, [55,56,22] or thermolysis at elevated temperatures [57,25,58,59,23].

Hydrolysis of ammonia borane can occur using a number of transition metals or their alloys [23,60-63] or acid catalyst [64,65] (Equations 2 and 3). A rapid hydrogen generation has been achieved by using the precious metal catalysts Pt, Rh, Ir, and Ru [23,66,67]. Hydrolysis of ammonia borane allows for the generation of

three equivalents of hydrogen gas per equivalent of ammonia borane and is faster than thermal degradation. The disadvantage of the hydrolysis mechanism for hydrogen release is the inability to recycle the fuel. While AB is long term stable in pure water, [23] the catalytic hydrolysis of AB results in ammonium metaborate according to below equations.

$$H_3NBH_3 + H^+ + 3H_2O \longrightarrow NH4^+ + B(OH)_3 + 3H_2 \quad (2)$$

$$H_3NBH_3 + 2H_20 \xrightarrow{\text{metal catalyst}} NH_4^+ + BO_2^- + 3H_2 \quad (3)$$

A catalyst is vital to have a practical application for effective hydrogen production from AB. The catalyst that will be used must be economic and should change the rate and effectiveness of the reaction significantly. Other properties that must be improved for effective use of AB in fuel cell applications are that the reactions which generate hydrogen must be recyclable and the reaction should not evaluate ammonia (NH_3) gas.

CHAPTER 3

3. TRANSITION METAL(0) NANOCLUSTERS

3.1. General Introduction

Nanoclusters are monodispersed particles that are generally less than 10 nm (100 A°) in diameter [68] have generated intense interest over the past decade. One reason for this is the belief that nanoclusters will have unique properties, derived in part from the fact that these particles and their properties lie somewhere between those of bulk and single-particle species [69,70]. Nanoparticles have many fascinating potential uses, including quantum dots [71] or quantum computers [72] and devices [73,74], chemical sensors [75], light-emitting diodes [76], 'ferrofluids' for cell separations [77], industrial lithography [78], and photochemical pattern applications such as flat-panel displays [79]. Nanoclusters also have significant potential as new types of higher activity and selectivity catalysts [80].

Two reasons chemists believe that nanoclusters hold the potential to be more active and selective catalysts than those of today are that a large percentage of a nanoclusters' metal atoms lie on the surface, and that surface atoms do not necessarily order themselves in the same way that those in the bulk do [81]. Furthermore, the electrons in nanoclusters are confined to spaces that can be as small as a few atom-widths across, giving rise to quantum size effects [81]. Perhaps most importantly, nanoclusters offer the possibility of controlling both the nanocluster size

and the surface ligands in a quantitative, modifiable and better understood way than previously possible for, say, supported heterogeneous catalysts.

Metal nanoclusters have unique and interesting physical and chemical properties. This can be observed in Figure 3.1.1. showing that the large numbers of the metal atoms lie on the surface, which means that the decrease in particle size causes the increasing in the number of the atoms on surface. Besides, the surface atoms do not necessarily order themselves in the same way that those in the bulk do [81].

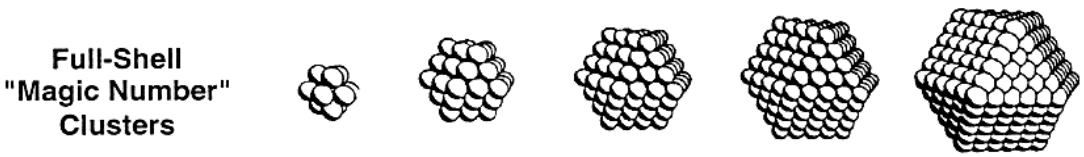

Full-Shell "Magic Number" Clusters					
Number of shells	1	2	3	4	5
Number of atoms in cluster	M_{13}	M_{55}	M_{147}	M_{309}	M_{561}
Percentage surface atoms	92%	76%	63%	52%	45%

Figure 3.1.1. The relation between the total number of atoms in full shell clusters and the percentage of surface atoms [82].

In nanoclusters, the bands theory of solid has inconvenient features because of the decreasing in the number of aggregated atoms, which leads to rise the gaps between their energy levels, as shown in figure 3.1.2., as well as the varying in their electric conductive properties [83], this phenomenon is known as ‘energy level quantization’ [84, 85, 86]. In another way, nanoclusters have size dependent optical properties, due to the variation in the mobility electrons located on (or near) to the surface (interface) with varying of their sizes [87,85,86,88].

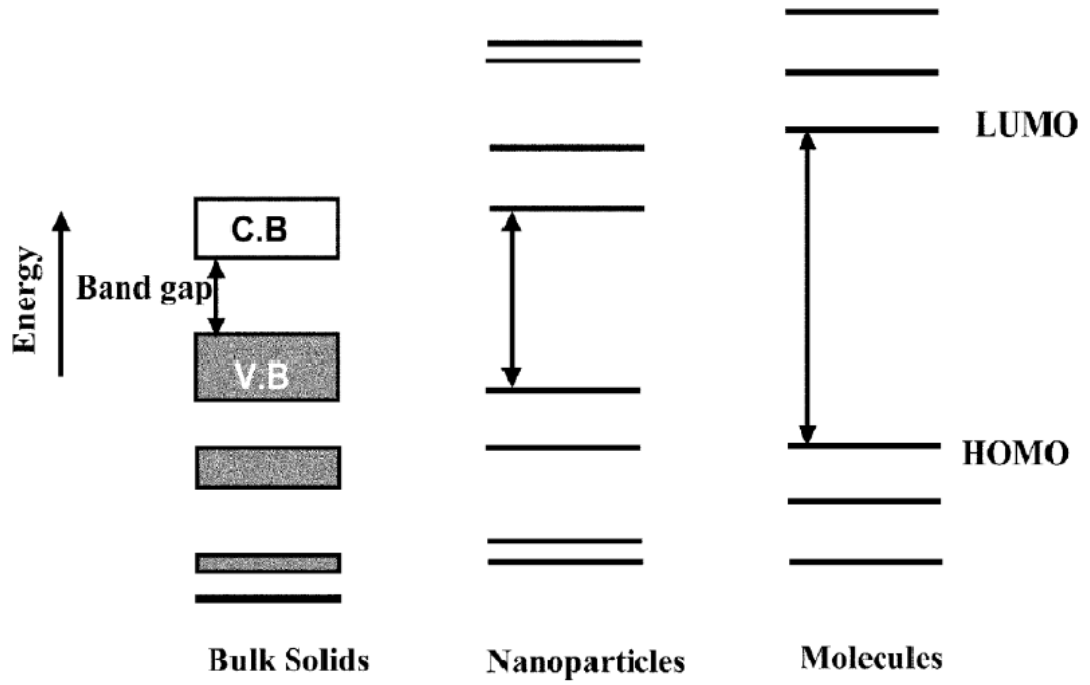

Figure 3.1.2. Schematic image describes the difference between energy levels of the bulk, nanoparticles and molecules. [85].

3.2. Stabilization of Transition Metal(0) Nanoclusters

One of the main characteristics of colloidal particles is their small size. Unfortunately, these metallic nanoparticles are unstable with respect to agglomeration to the bulk. In most cases, this aggregation leads to the loss of the properties associated with the colloidal state of these metallic particles. For example, during catalysis the coagulation of colloidal particles used as catalyst leads to a significant loss of activity. The stabilization of metallic colloids and thus the means to preserve their finely dispersed state is a crucial aspect to consider during their synthesis. Several general discussions on the stability of colloids and nanoclusters have been already reported [89,90,68,30,91-96]. The general stabilization mechanisms of colloidal materials have been described in Derjaguin-Landau-

Verwey-Overbeek (DLVO) theory [97]. Nanocluster stabilization is usually discussed in terms of three general categories: i) electrostatic stabilization, ii) steric stabilization, iii) electrosteric stabilization.

3.2.1. Electrostatic Stabilization

Ionic compounds such as halides, carboxylates, or polyoxoanions, dissolved in (generally aqueous) solution can generate the electrostatic stabilization. The adsorption of these compounds and their related counterions on the metallic surface will generate an electrical double-layer around the particles (Figure 3.2.1.1.). This results in a Coulombic repulsion between the particles. If the electric potential associated with the double layer is high enough, then the electrostatic repulsion will prevent particle aggregation [89, 90, 94, 98].

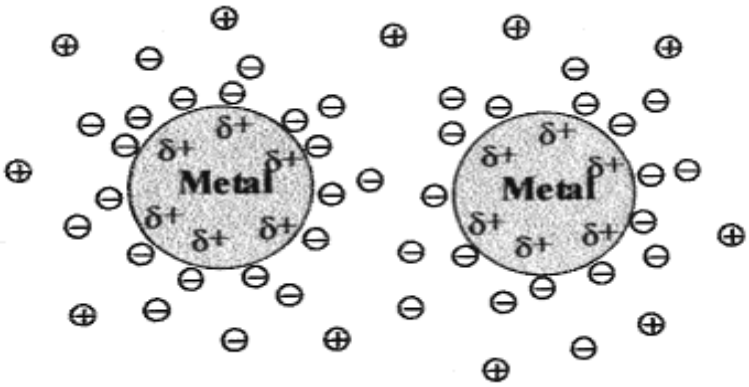

Figure 3.2.1.1. Schematic representation of electrostatic stabilization of metal colloid particles.

3.2.2. Steric Stabilization

A second means by which metal colloids can be prevented from aggregating is to use macromolecules such as polymers or oligomers [94,99]. The adsorption of these molecules at the surfaces of the particles will provide a protective layer. The

way in which these large adsorbed molecules prevent aggregation can be explained in a simplified manner by visualizing the approach of two metallic colloids. In the interparticle space, adsorbed molecules will be restricted in motion, which causes a decrease in entropy and thus an increase in free energy (Figure 3.2.2.1.).

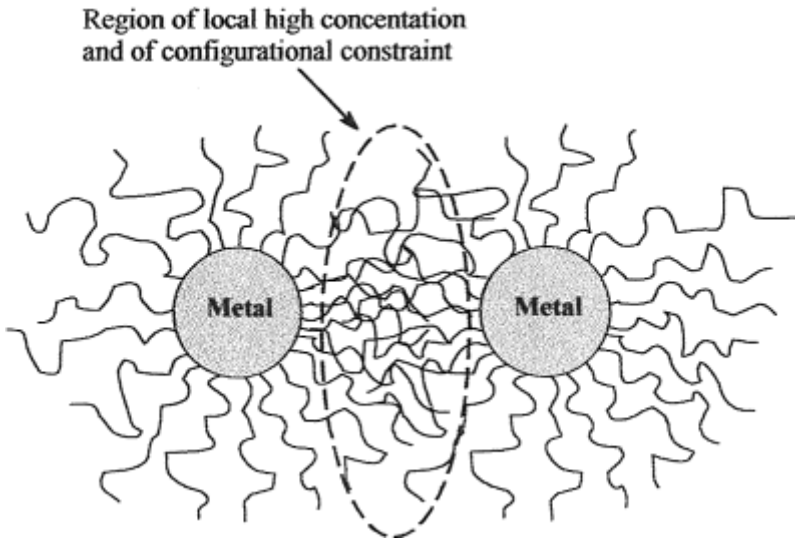

Figure 3.2.2.1. Schematic representation of steric stabilization of metal colloid particles.

3.2.3. Electrosteric Stabilization

The electrostatic and steric stabilization can be combined to maintain metallic nanoparticles stable in solution [68,100]. This kind of stabilization is generally provided by means of ionic surfactants. They can generate a polar head group which can create electrical double layer and a lypophilic side chain which can provide steric repulsion as shown in figure 3.2.3.1. At the time two particles approach each other, both electrostatic repulsion and steric limitation prevent agglomeration of nanoparticles.

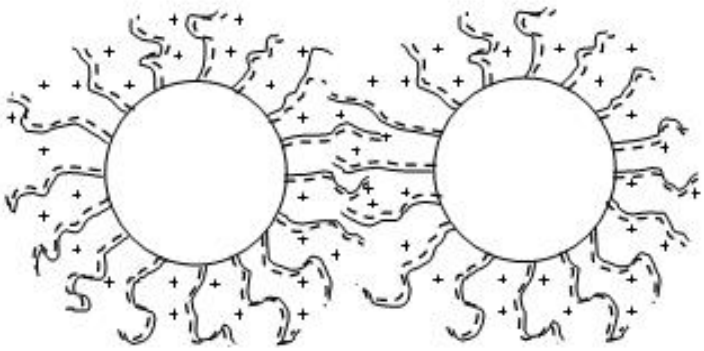

Figure 3.2.3.1. Representation of the electrosteric stabilization of nanoparticles in solution [99].

3.3. Preparation of Transition Metal (0) Nanoparticles

Nanoparticles whose particle size deviates less than 10% from the average value are generally addressed as ‘monodisperse’. A deviation from the mean particle size of approximately 20% is described as showing a ‘narrow size distribution’. The synthesis is expected to be a crucial point in producing nanoparticles with defined properties. Nanoparticles have been obtained by two different approaches, which are called "top-down" (from large to small dimensions) and "bottom up" (from molecular scale to nanoscale) methods. A common "top-down" approach involves breaking bulk materials to nanometer-sized particles. This process is generally associated with the use of mechanical force, such as grinding and ball milling. Though this approach is easy for large scale production, size distribution of particles obtained is broad.

A large variety of nanoparticles can be synthesized via the "bottom up" approach, which relies on chemical methods. In general these methods can be divided into five main categories as: (i) the chemical reduction of transition-metal

salts [101], (ii) the electrochemical reduction of transition metal salts [102], (iii) thermal or photochemical decomposition of transition-metal precursors [103], (iv) ligand reduction and displacement from organometallic compounds [104], and (v) metal vapor synthesis [105]. Some synthetic techniques use a combination of these five methods. Of the five methods, the chemical reduction of transition-metal salts is by far the most common.

3.4. Characterization of Transition Metal (0) Nanoparticles

A key goal of nanocluster characterization is to establish particle size and overall composition. Surface composition is sometimes also probed, but this is a more formidable task. Fig. 3.4.1. provides a good overall picture of the techniques most often used to characterize nanoclusters [106].

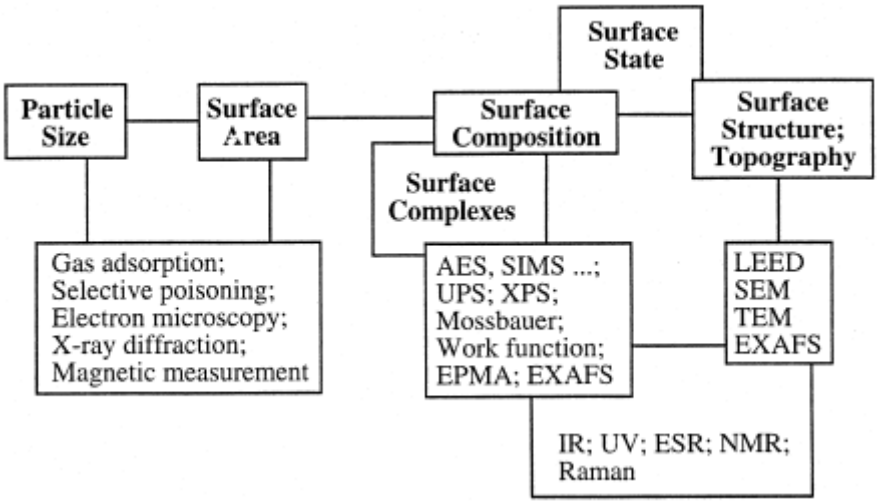

Figure 3.4.1. Common methods available for the characterization of nanoclusters, adapted from Ref. [106].

The most widely used technique for characterizing nanoparticles is transmission electron microscopy (TEM) or high resolution TEM (HRTEM),

techniques which provide direct visual information on the size, shape, dispersity, structure, and morphology of nanoclusters [107]. Another method giving information about size of a nanoparticle is X-Ray electron diffraction (XRD) technique. Using peak features and Debye-Scherrer equation one can calculate the approximate nanoparticle size. In addition, X-Ray photoelectron spectroscopy (XPS) can be used to investigate elements and their distribution on surface of metal NPs stabilized on a support or present in powder form; besides, chemical and electronic state are investigated. Other commonly used methods for characterization of metal particles include UV-Visible spectroscopy (UV–Vis), nuclear magnetic resonance spectroscopy (NMR), infrared spectroscopy (IR), elemental analysis, and energy dispersive spectroscopy (EDS). To a lesser extent the following methods are used: analytical ultracentrifugation–sedimentation, extended X-ray absorption fine structure (EXAFS), scanning tunneling microscopy (STM), atomic force microscopy (AFM), high performance liquid chromatography (HPLC), light scattering, time of flight mass spectrometry, magnetic susceptibility, and electrophoresis or ion-exchange chromatography [90].

3.5. Transition Metal (0) Nanoclusters in Catalysis

3.5.1. General Principles of Catalysis

The first introduction of the word ‘catalysis’ was by Berzelius in 1836, while Ostwald presented the first correct definition of a catalyst in 1895. He described a catalyst as a substance that changes the rate of a chemical reaction without itself appearing in the products. Since then catalysis has gained an increasing importance and has been closely related to our daily lives. Almost 80% of all chemicals

produced in the chemical industry have been in contact with one or more catalysts. While only a very small portion of the world production is spent on catalysts, almost 25% of the world production is achieved with the aid of catalysts.

A catalyst accelerates a chemical reaction. It does so by forming bonds with the reacting molecules (i.e. adsorption), such that they can react to a particular product, which detaches itself from the catalyst (i.e. desorption), and leaves the catalyst unaltered so that it is ready to interact with the next set of molecules. A catalyst cannot alter the chemical equilibrium of a given reaction; it only creates a favorable reaction pathway. In order for a reaction to take place some requirements must be fulfilled regarding the molecules that react. As the reactants must come in contact, they must have or gain the energy to overcome the activation barrier (the activation energy) and they must also be correctly oriented relative to one another. A catalyst is said to lower the activation energy of the reaction by providing a different transition state, illustrated in figure 3.5.1.1. (exothermic reaction).

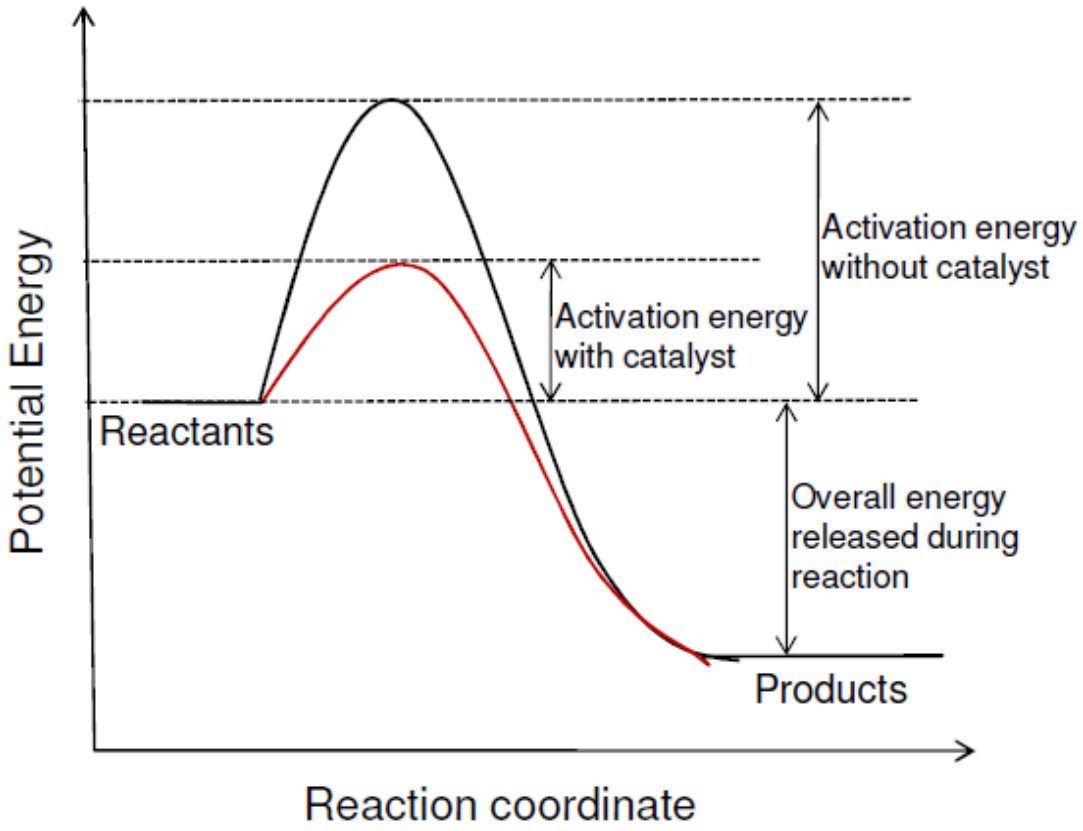

Figure 3.5.1.1. Energy diagram of an exothermic chemical reaction illustrating the difference in activation energy between an uncatalyzed and a catalyzed reaction.

As a result, catalysts can make reactions occur at lower temperatures and pressures and with increased reaction rates and selectivity. Therefore, catalytic processes are significant in the efforts to meet the demands and requirements of environmentally friendly processes in the industrial chemistry.

Three main properties of a catalyst are activity, stability, and selectivity. The *total turnover number* (TTON) is calculated to determine activity of a catalyst. TON is the number of moles of substrate that a mole of catalyst can convert before becoming inactivated. Total turnover number (TTON) is the number of moles of product per mole of catalyst.

$$TTON = \frac{mol\ of\ product}{mol\ of\ catalyst} \tag{4}$$

The turnover frequency (TOF) is the important for the catalytic efficiency. For the conversion of A to the product B in the presence of catalyst with a rate of *v,* the following relation can be expressed for turnover frequency (eqn (5)).

$$A \xrightarrow{\text{catalyst}} B$$

$$v = \frac{d[B]}{dt}$$

$$TOF = \frac{v}{catalyst} \tag{5}$$

Most important attribute is the selectivity of catalyst, which reflects its ability to direct conversion of the reactant(s) along one specific pathway [108].A selective catalyst yields a proportion of the desired product with minimum amounts of side products. In industry, there is considerable economic incentive to develop selective catalysts [109].

The last property is the chemical, thermal and mechanical stability of a catalyst determine its lifetime in industrial reactors. Deactivation of the catalyst caused by aging or poisoning can be affected stability of catalyst.

3.5.2. Classification of Catalysts

Catalysis can be classified into three groups as homogeneous, heterogeneous and biocatalysts.

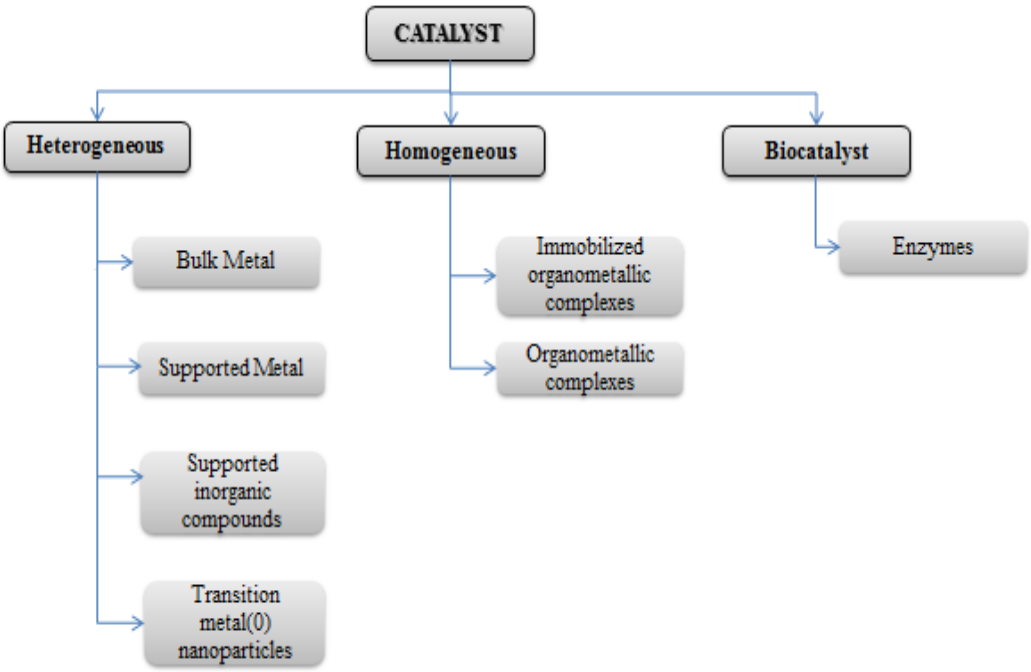

Figure 3.5.2.1. The classification of catalysts [67]

Homogeneous catalysis where the reactant molecules and the catalyst are present in a single phase, as in a liquid solution. In the specific case of homogeneous transition metal catalysis, the solubility and resulting ability to study the catalysis in detail allows for the careful tailoring of catalyst properties. Such catalyst systems offer many avenues for the detailed control of reactivity. In heterogeneous catalysis, where the reactants are present in one phase and the catalyst in another. Heterogeneous catalysts tend to offer greatly enhanced thermal stability. Furthermore, catalyst separation from the reaction vessel is unproblematic. Separation may be performed by simple filtration resulting in products which display very low trace metal contamination. Heterogeneous catalysis affects our daily lives. More than 80% of industrial chemical processes in use nowadays rely on one or more catalytic reactions. A number of those, including oil refining, petrochemical processing and the manufacturing of commodity chemicals (e.g. olefins, methanol, ethylene glycol) are already well established [111]. Heterogeneous catalysis is

associated with the production of petro- and bulk chemicals whereas fine and specialty chemicals are produced predominantly with non-catalytic organic synthesis [112]. Third group is biocatalysts. Most of the reactions that occur in living organisms are catalysed by molecules called enzymes. Most enzymes are proteins, which are formed from amino acid monomers. Enzymes regulate virtually all the reactions in biology [113].

CHAPTER 4

4. EXPERIMENTAL SECTION

4.1. Materials

Rhodium(III) chloride trihydrate ($RhCl_3 \cdot 3H_2O$), titanium(IV) oxide (anatase), and ammonia-borane (AB, 97%) were purchased from Aldrich and used without further purification. Deionized water was distilled by water purification system (Milli-Q System). All glassware and Teflon-coated magnetic stir bars were cleaned with acetone, followed by copious rinsing with distilled water before drying in an oven at 150ºC.

4.2. Characterization

The rhodium content of the $Rh(0)@TiO_2$ sample was determined by Inductively Coupled Plasma Optical Emission Spectroscopy (ICP-OES, Leeman-Direct Reading Echelle) after the sample was completely dissolved in the mixture of HNO_3/HCl (1/3 ratio). Transmission electron microscopy (TEM) was performed on a JEM-2100F (JEOL) microscope operating at 200 kV. A small amount of powder sample was placed on the holey carbon grid of the transmission electron microscope. Samples were examined at magnification between 100 and 400 K. Scanning electron microscope (SEM) images were taken using a JEOL JSM-5310LV at 15 kV and 33

Pa in a high-vacuum mode without metal coating on carbon support. The X-ray photoelectron spectroscopy (XPS) analysis was performed on a Physical Electronics 5800 spectrometer equipped with a hemispherical analyzer and using monochromatic Al Kα radiation of 1486.6 eV, the X-ray tube working at 15 kV, 350W and pass energy of 23.5 keV. ^{11}B-NMR spectra were recorded on a Bruker Avance DPX 400 with an operating frequency of 128.15 MHz for ^{11}B.

4.3. Preparation of rhodium(III) ions impregnated on TiO_2

TiO_2 (1000 mg) was added to a solution of $RhCl_3 \cdot 3H_2O$ (53.97 mg) in 100 mL H_2O in a beaker. This slurry was stirred at room temperature for 72 h and then $Rh^{3+}@TiO_2$ sample was isolated by centrifugation and washed with 100 mL of distilled water and the remnant was dried at 120^{o}C for 12 h in an oven.

4.4. In situ formation of rhodium(0) nanoparticles supported on TiO_2 and concomitant catalytic hydrolysis of AB

Rhodium(0) nanoparticles supported on TiO_2 (Rh(0)@TiO_2) were *in situ* generated from the reduction of $Rh^{3+}@TiO_2$ during the catalytic hydrolysis of AB. Before starting the catalyst formation and concomitant catalytic hydrolysis of AB, a jacketed reaction flask (20 mL) containing a Teflon-coated stir bar was placed on a magnetic stirrer (Heidolph MR-301) and thermostated to 25.0 ± 0.1°C by circulating water through its jacket from a constant temperature bath. Then, a graduated glass tube (60 cm in height and 3.0 cm in diameter) filled with water was connected to the reaction flask to measure the volume of the hydrogen gas to be evolved from the reaction. (Figure 4.4.1.)

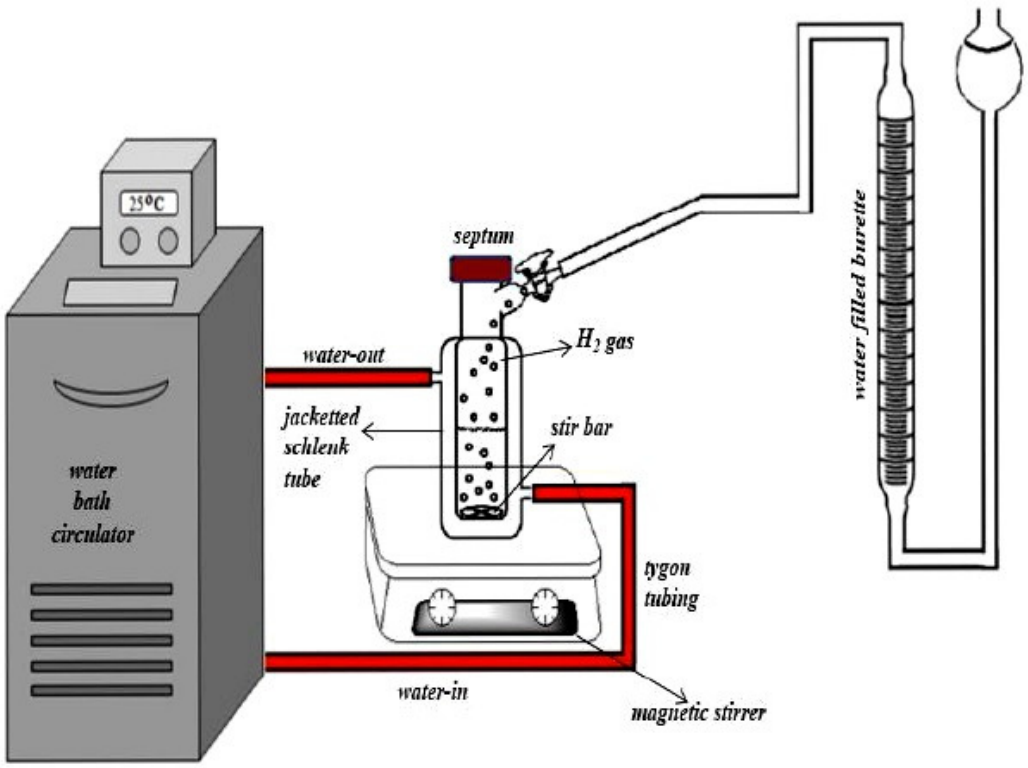

Figure 4.4.1. Experimental set-up used for determining hydrogen gas generation during reactions and also to study kinetic experiments.

Next, 20 mg powder of $Rh^{3+}@TiO_2$ (0.24 wt.% Rh) was dispersed in 10 mL distilled water in the reaction flask thermostated at 25.0 ± 0.1°C. Then, 31.8 mg AB (1.0 mmol $H_3N.BH_3$) was added into the flask and the reaction mixture was stirred at 1000 rpm. After adding ammonia borane, rhodium(0) nanoparticles were formed and the catalytic hydrolysis of AB started immediately. The volume of hydrogen gas evolved was measured by recording the displacement of water level every 30 sec. at constant atmospheric pressure of 693 Torr. The reaction was stopped when no more hydrogen evolution was observed. In each experiment, the resulting solutions were filtered and the filtrates were analyzed by ^{11}B-NMR and conversion of AB to metaborate anion was confirmed by comparing the intensity of signals in the ^{11}B-NMR spectra of the filtrates.

4.5. Kinetic Studies for Rh(0)@TiO_2 Catalyzed Hydrolysis of Ammonia-Borane

In order to determine the rate law of Rh@TiO_2 catalyzed hydrolysis of ammonia-borane, two different sets of experiments were performed. In the first set, the concentration of rhodium was kept constant at 0.116 mM (50 mg Rh^{3+}@TiO_2 in 10 mL) meanwhile the NH_3BH_3 concentration was altered as 50, 100, 200, and 300 mM (15.9, 31.8, 63,6 and 95.4 mg NH_3BH_3 respectively). In the second set, the ammonia-borane concentration was kept constant at [NH_3BH_3] = 100 mM (31.8 mg NH_3BH_3) and rhodium concentration was changed as 0.023, 0.046, 0.116, and 0.233 mM (10, 20, 50 and 100 mg Rh^{3+}@TiO_2, respectively).

4.6. Determination of activation energy for hydrolysis of AB catalyzed by Rh(0)@TiO_2

In a typical experiment, the hydrolysis reaction was performed starting with 10 mL of 100 mM (31.8 mg) AB solution and 20 mg Rh^{3+}@TiO_2 (0.24% wt. rhodium, [Rh] = 0.046 mM) at various temperatures (25, 30, 35, 40, 45°C) in order to obtain the activation energy. The values of the observed rate constants k_{obs} for the hydrolysis of NH_3BH_3 were determined for each temperature and utilized to calculate the activation energy by using Arrhenius plot.

4.7. Reusability of Rh(0)@TiO_2 in hydrolysis of AB

After the complete hydrolysis of AB started with 10 mL of 100 mM AB (31.8 mg H_3NBH_3), and 100 mg Rh^{3+}@TiO_2 (0.24 % wt. Rhodium, [Rh] = 0.233 mM) at 25 ± 0.1°C, the catalyst was isolated as a powder by centrifugation and dried at 120°C in the oven after washing with 20 mL of water. The isolated samples of Rh(0)@TiO_2 were weighed and redispersed in 10 mL solution of 100 mM AB for a subsequent run of hydrolysis at 25 ± 0.1°C.

4.8. Determination of the catalytic lifetime of Rh(0)@TiO_2 in the hydrolysis of AB

The catalytic lifetime of Rh(0)@TiO_2 in the hydrolysis of AB was determined by measuring the total turnover number (TTO). Such a lifetime experiment was started with a 50 mL solution containing 0.046 mM Rh(0)@TiO_2 and 30 mM AB at 25.0 ± 0.1°C. When all the ammonia-borane present in the solution was completely hydrolyzed, more AB was added and the reaction was continued in this way until no hydrogen gas evolution was observed.

CHAPTER 5

5. RESULTS AND DISCUSSIONS

5.1. Preparation and characterization of Rhodium (0) Nanoparticles Supported on TiO_2

Rhodium(0) nanoparticles supported on titanium dioxide were *in situ* generated from the reduction of $Rh^{3+}@TiO_2$ during the catalytic hydrolysis of AB. Rhodium(III) ions were first impregnated on titania with particle size of 100 nm from the aqueous solution of rhodium(III) chloride yielding $Rh^{3+}@TiO_2$ and then reduced by AB at room temperature. Both reduction of rhodium(III) to rhodium(0) and hydrogen release from the hydrolysis of AB, occur concomitantly when AB solution is added to a suspension of $Rh^{3+}@TiO_2$. The progress of the AB hydrolysis was followed by monitoring the change in hydrogen pressure which was then converted into the equivalent H_2 per mole of AB, using the known 3:1 H_2/AB stoichiometry (eq 1)(p:3)

Rhodium(0) nanoparticles supported on titania ($Rh(0)@TiO_2$), *in situ* formed during the hydrolysis of AB, could be isolated from the reaction mixture as powder by centrifugation and then characterized by ICP-OES, XRD, SEM-EDS, TEM, XPS and N_2 adsorption-desorption techniques. Rhodium content of $Rh(0)@TiO_2$ was determined by inductively coupled plasma optical emission spectroscopy (ICP-OES)

and found as 0.24% wt. Rh loading on titania surface. The N_2 adsorption-desorption analysis gave the surface area of titania as 10.71 m^2/g. Since the rhodium content of Rh(0)@TiO_2 was very low, it was difficult to detect the existence of rhodium(0) nanoparticles on the surface of titania by N_2 adsorption-desorption analysis. Comparison of the XRD patterns of TiO_2, Rh^{3+}@ TiO_2 and Rh(0)@TiO_2 with a rhodium loading of 0.24 wt.% Rh, given in Figures 5.1.1.a, 5.1.1.b, and 5.1.1.c, respectively show that there is no change in the characteristic diffraction peaks of TiO_2 (JCPDS Card 21-1272).

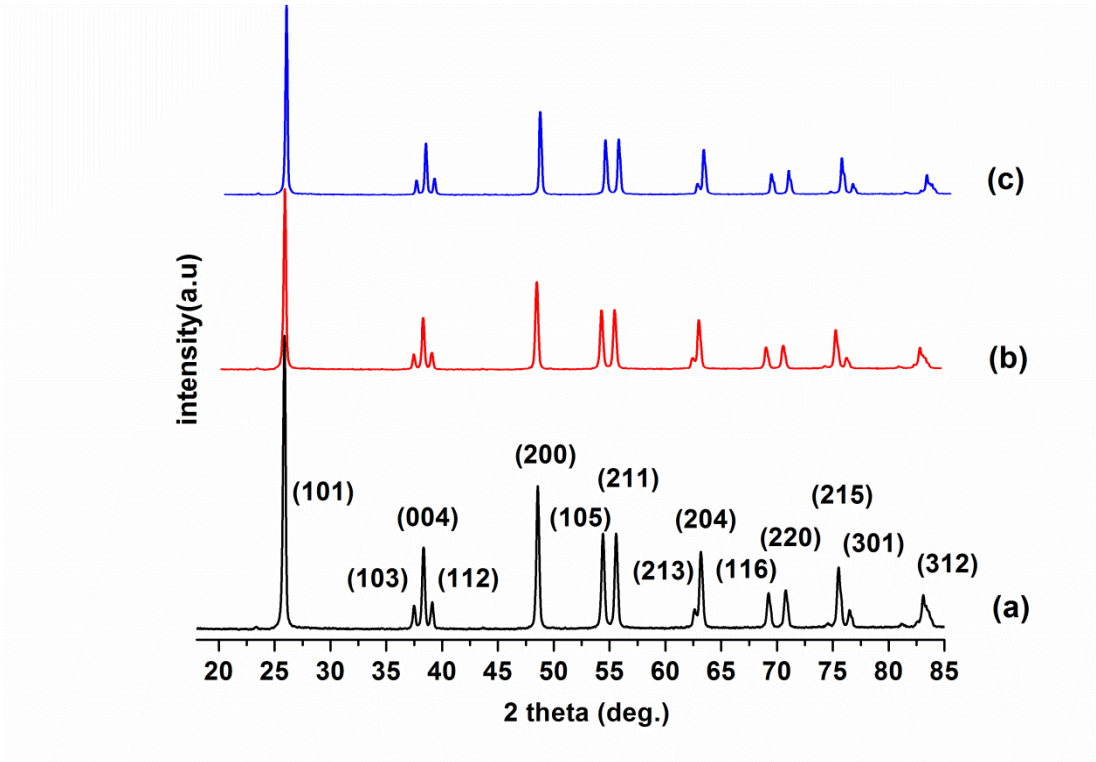

Figure 5.1.1. Powder X-ray diffraction (PXRD) patterns of (a) TiO_2, (b) Rh^{3+}@TiO_2, (c) Rh(0)@TiO_2 with a 0.24% wt. Rh loading.

According to the result of the powder X-ray diffraction patterns of TiO_2, Rh^{3+}@TiO_2 and Rh(0)@TiO_2, the host material remains intact after impregnation and reduction of rhodium(III) ions; there is no noticeable alteration in the framework lattice or change in the crystallinity. There is no observable peak attributable to

rhodium nanoparticles in Figure 5.1.1.b and 5.1.1.c, probably because of low rhodium loading of TiO_2.

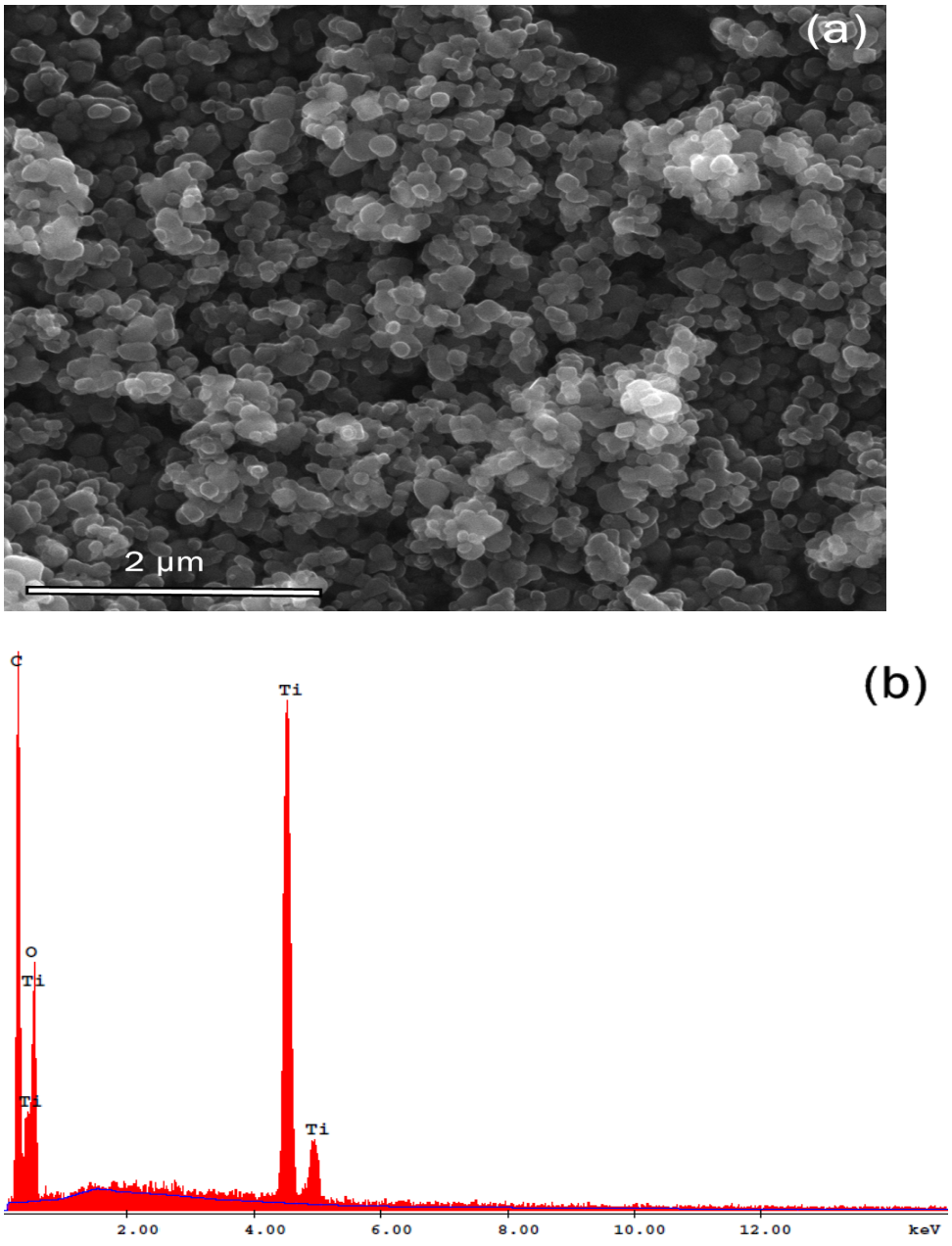

Figure 5.1.2. (a) Scanning Electron Microscopy (SEM) image and (b) SEM-EDS spectrum of Rh(0)@TiO_2 with a 0,24% wt. Rh loading

The next technique used was scanning electron microscopy (SEM) giving information about surface of the prepared catalyst. SEM image of Rh(0)@TiO_2 with

a rhodium loading of 0.24% wt. given in Figure 5.1.2.a shows the presence of nearly monodispersed titania nanoparticles of 100 nm size. The SEM-EDS spectrum of Rh(0)@TiO_2 with a rhodium loading of 0.24% wt. (in Figure 5.1.2.b) indicates the presence of the framework elements of TiO_2 (Ti, O). Because of the low rhodium loading on TiO_2, the presence of rhodium nanoparticles could not be observed in SEM analysis.

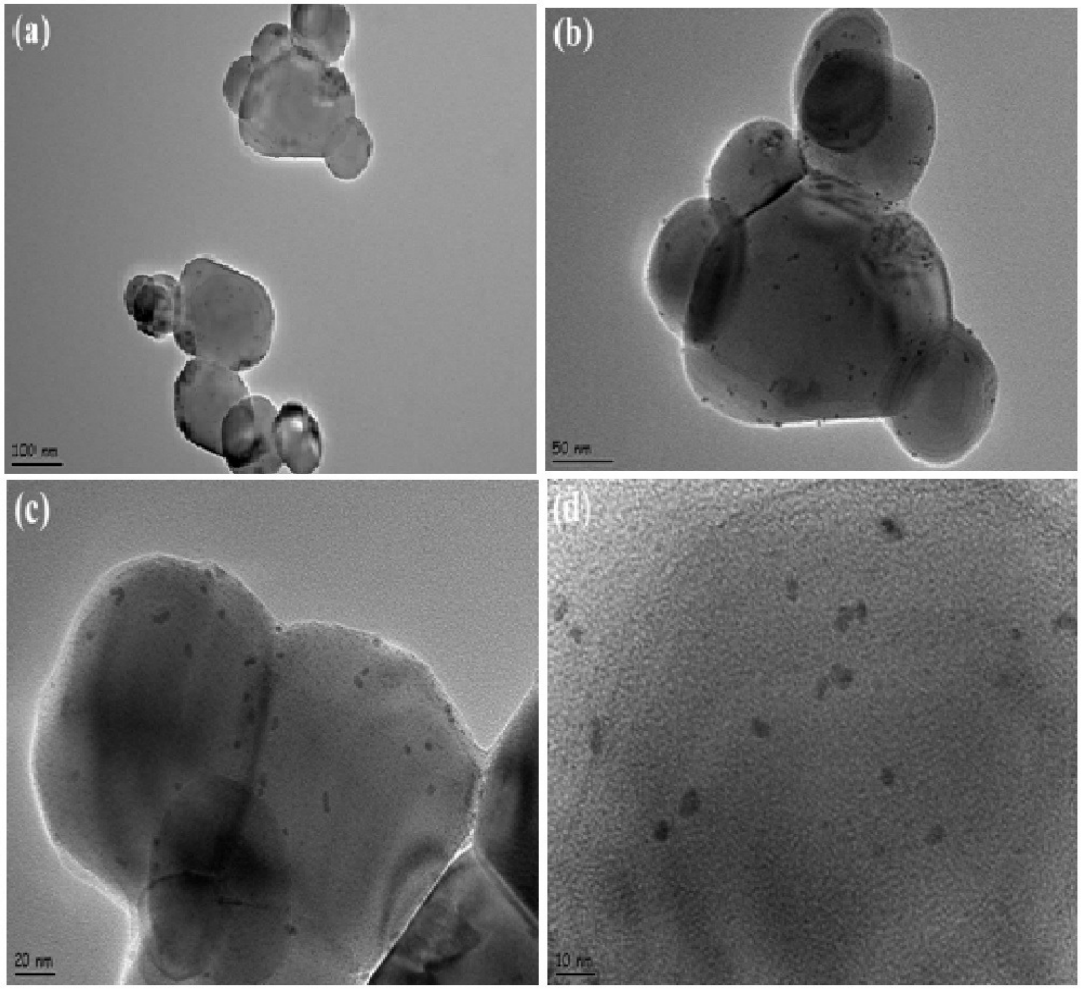

Figure 5.1.3. Transmission Electron Microscopy (TEM) images of Rh(0)@TiO2 with a rhodium loading of 0.24% wt. at (a) 100 nm, (b) 50 nm, (c) 20 nm, (d) 10 nm

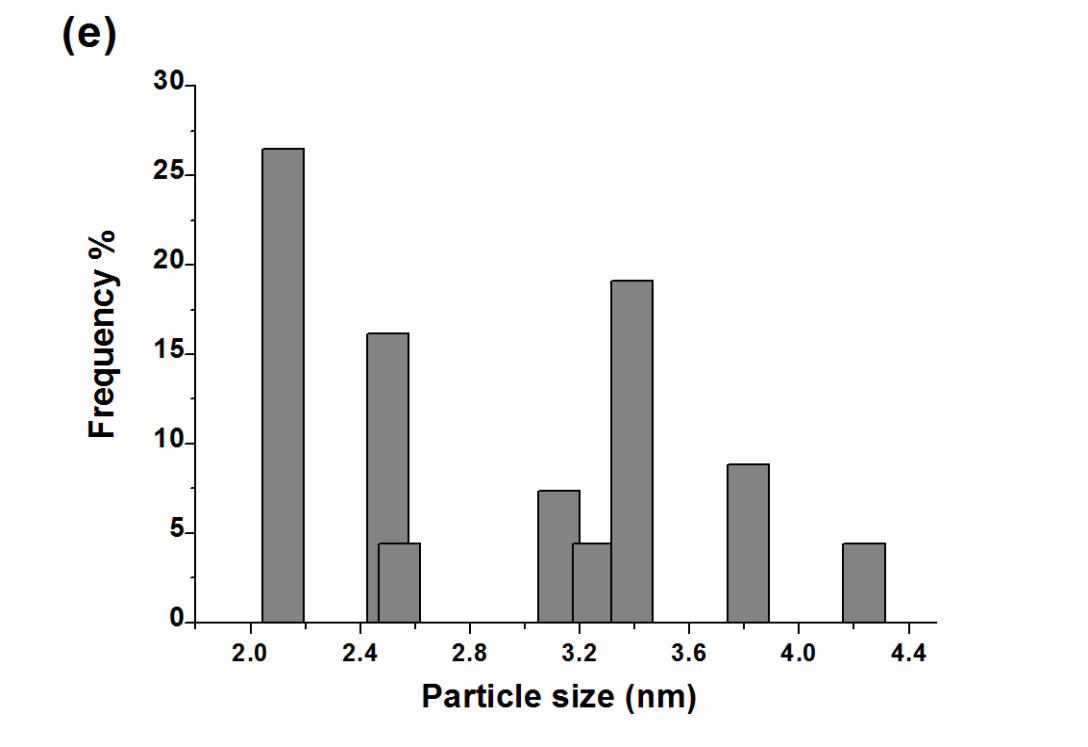

Figure 5.1.3. (continued) (e) Histogram of Rh(0)@TiO_2 showing particle size distribution.

One of the most efficient methods in characterization of the metal nanoparticles is the transmission electron microscopy (TEM). From which one can easily have enough information about size, shape, and size distribution of nanoparticles. Figure 5.1.3. shows the TEM images of Rh(0)@TiO_2 with a rhodium loading of 0.24% wt. taken with different magnifications. The Figure 5.1.3. indicates that (*i*) highly dispersed rhodium(0) nanoparticles are formed on the surface of TiO_2 with particle size in the range 1.3-3.8 nm (mean diameter: 2.8 ± 0.7 nm) and (*ii*) the impregnation of rhodium(III) followed by reduction to rhodium(0) causes no change in the framework lattice of titania. This result is in good agreement with the XRD results.

The composition of Rh(0)@TiO_2 formed *in situ* during the hydrolysis of AB and the oxidation state of rhodium were also studied by XPS technique.

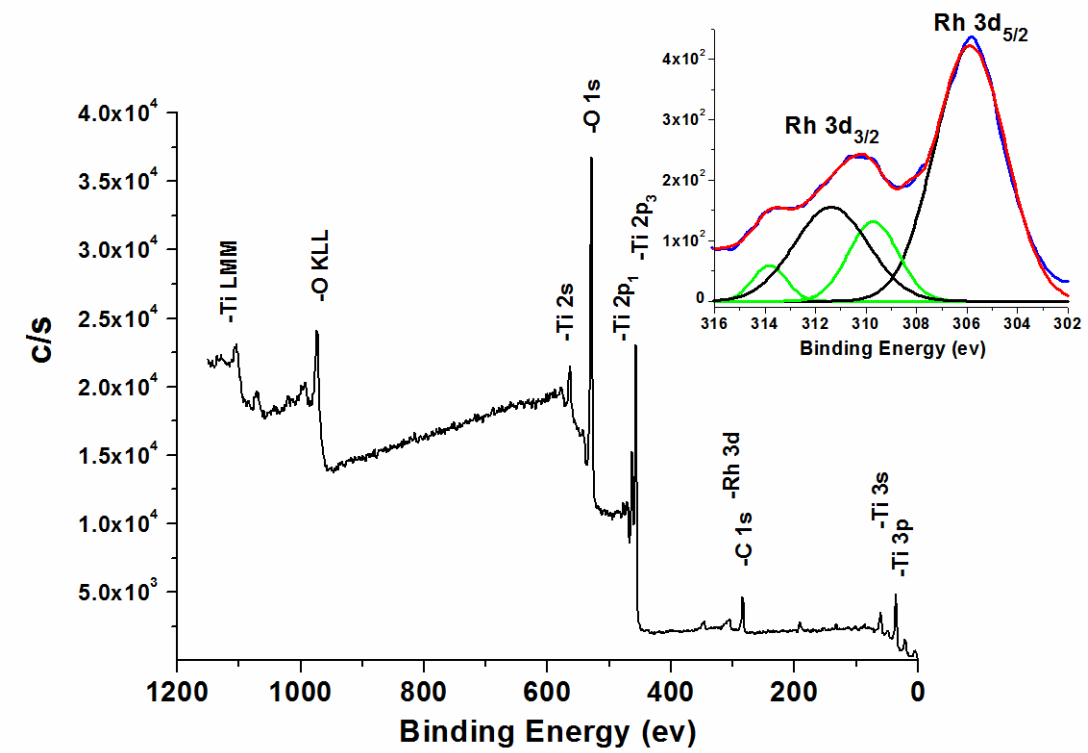

Figure 5.1.4. X-ray photoelectron (XPS) spectrum of Rh(0)@TiO_2 sample with a rhodium loading of 0.24% wt. Rh. The inset gives the high resolution scan and deconvolution of Rh 3d bands.

The survey-scan XPS spectrum of Rh(0)@TiO_2 with a rhodium loading of 0.24% wt. (Fig. 5.1.4.) shows that rhodium is the only element detected in addition to the TiO_2 framework elements (Ti, O). High resolution Rh 3d XPS of a Rh(0)@TiO_2 sample given in the inset of Figure 5.1.4. shows two prominent bands at 305.8 eV and 311.4 eV which can readily be assigned to rhodium(0) $3d_{5/2}$ and $3d_{3/2}$, respectively [114,115]. The bands at 309.7 eV and 313.8 eV (in green color in the inset of Figure 5.1.4.), might be attributed to rhodium oxides, which might be formed during the XPS sampling [115].

5.2. Catalytic Activity of Rhodium(0) Nanoparticles Supported on Titania (Anatase) in the Hydrolysis of Ammonia-Borane.

Before starting with the investigation on the catalytic activity of Rh(0)@TiO_2 in the hydrolysis of AB, a control experiment was performed to check whether titanium dioxide shows any catalytic activity in the hydrolysis of AB at the same temperature used in this study. In a control experiment with a mixture of 1.0 mmol of AB and 20 mg of powder of TiO_2 (the same amount as the one used in catalytic activity tests) in 10 mL of water at 25.0 ± 0.1°C or 45.0 ± 0.1°C, there was no hydrogen evolution observed in 1 h at both temperatures. This observation indicates that the hydrolysis of AB does not occur in the presence of TiO_2 in the temperature range used in this study. However, Rh(0)@TiO_2 are found to be highly active catalyst in the hydrolysis of AB generating 3.0 equivalent H_2 gas per mole of AB in the same temperature range. In addition to the volumetric measurements of the hydrogen gas evolution, the completion of hydrolysis was investigated by using ^{11}B NMR spectroscopy. The ^{11}B NMR spectrum of pure ammonia borane recording from its D_2O solution shows the appearance of a quartet at -24.3 ppm (figure 5.2.1.a). After the hydrolysis, only one singlet at -9.9 ppm appeared (figure 5.2.1.b). This indicates the formation of metaborate ($NH_4(BO_2)$) after the hydrolysis reaction of ammonia borane.

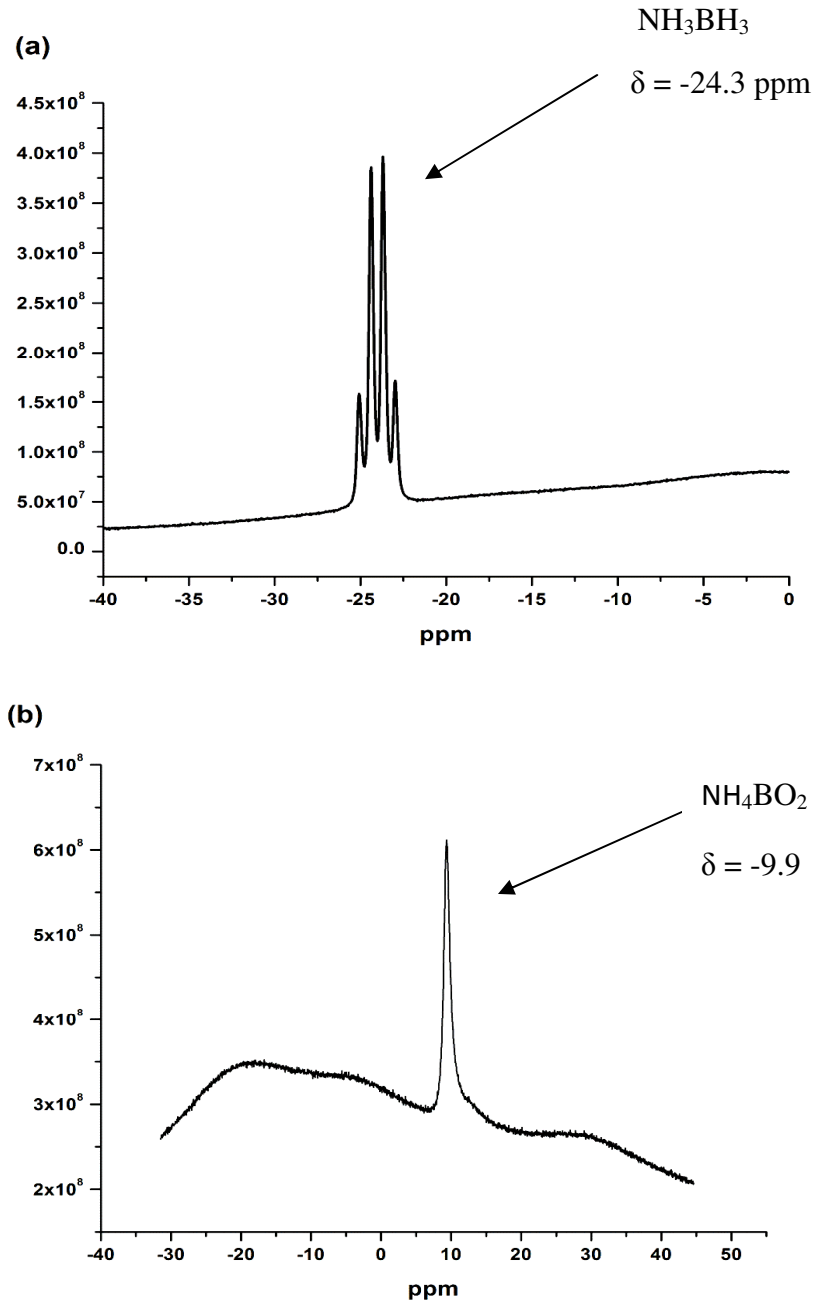

Figure 5.2.1. (a) ^{11}B NMR spectrum of AB before hydrolysis **(b)** after the completation of hydrolysis of AB.

Figure 5.2.2.a shows the evolution of equivalent hydrogen per mole of AB versus time plot for the hydrolysis of AB (100 mM) using Rh(0)@TiO_2 as catalyst in different rhodium concentration at 25.0 ± 0.1^oC. The hydrogen generation rate was determined from the linear portion of each plot. For all tests a complete hydrogen release (mol H_2/mol H_3NBH_3 = 3) was observed.

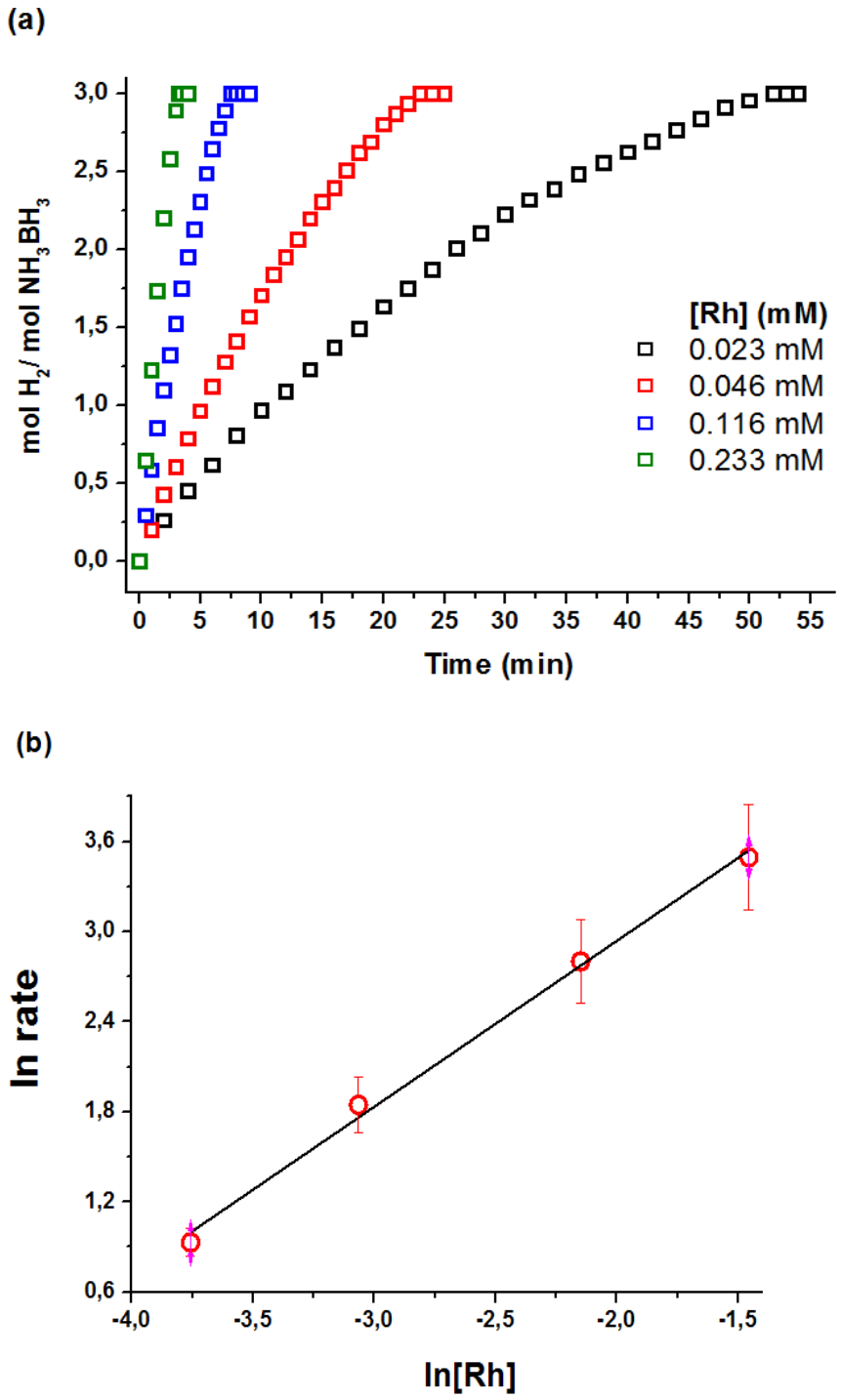

Figure 5.2.2. **(a)** mol H_2 /mol $H_3N.BH_3$ versus time graph depending on the rhodium concentration in Rh(0)@TiO_2 for the hydrolysis of AB (100 mM) at 25.0 ± 0.1°C, **(b)** The logarithmic plot of hydrogen generation rate versus the concentration of Rh; *ln*(rate) = 1.12 *ln*[Rh] + 4.34.

On the other hand, Figure 5.2.2.b shows the plot of hydrogen generation rate versus initial concentration of rhodium, both in logarithmic scale, which gives a straight line with a slope of 1.12 indicating that hydrolysis of AB is a first order with respect to the rhodium concentration. The turnover frequency (TOF), and mol of H_2 per mol of rhodium per minute, for hydrogen generation from the hydrolysis of AB (100 mM) at 25.0 ± 0.1°C was determined from the hydrogen generation rate in the linear portion of plots given in Figure 5.2.2.a for experiments starting with 100 mM AB plus Rh(0)@TiO_2 with a loading of 0.24% wt. Rh. The TOF value of Rh(0)@TiO_2 catalyst is as high as 260 min^{-1} (mol H_2/mol Rh.min) in hydrolysis of AB at 25.0 ± 0.1°C. For comparison the TOF values of the reported catalysts used in the hydrolysis of AB are listed in Table 1. As it is seen from the comparison of values listed in Table 1, Rh(0)@TiO_2 provide remarkable TOF value in the hydrolysis of AB as compared to the other ruthenium, rhodium and palladium catalysts.

Table 1: Catalytic activity of reported various catalysts used in the hydrolysis of AB

Entry	Catalyst	TOF (min^{-1})	Ea (kj/mol)	TTO	Ref
1	Ru@MWCNT	329	33	26.4	116
2	Rh(0)@TiO_2	260	65.5	37.35	117
3	Laurate-stabiliz	200	43.6	80	118
4	Ru(0)PSSA-co-l	172	54	51.72	119
5	Ru(0)@Hap	137	58	87	120
6	Ni@Ru	114	44	-	121
7	Ru/Carbon	113	76	-	61
8	Ru/Graphene	100	11.7	-	122
9	ZFS Rh(0)	92	66.9	47.2	66
10	RuNPs@ZK-4	90.2	28	36.7	123
11	Ru(0)NP/Laurat	75	47	5.9	67
12	Pd@Co/graphe	37.5	-	-	124
13	$Co_{35}Pd_{65}$/C anne	35.7	-	-	125
14	2.1 wt% RGO@	23.3	40	-	126
15	Rh/γ-Al_2O_3	-	21	-	23(f)

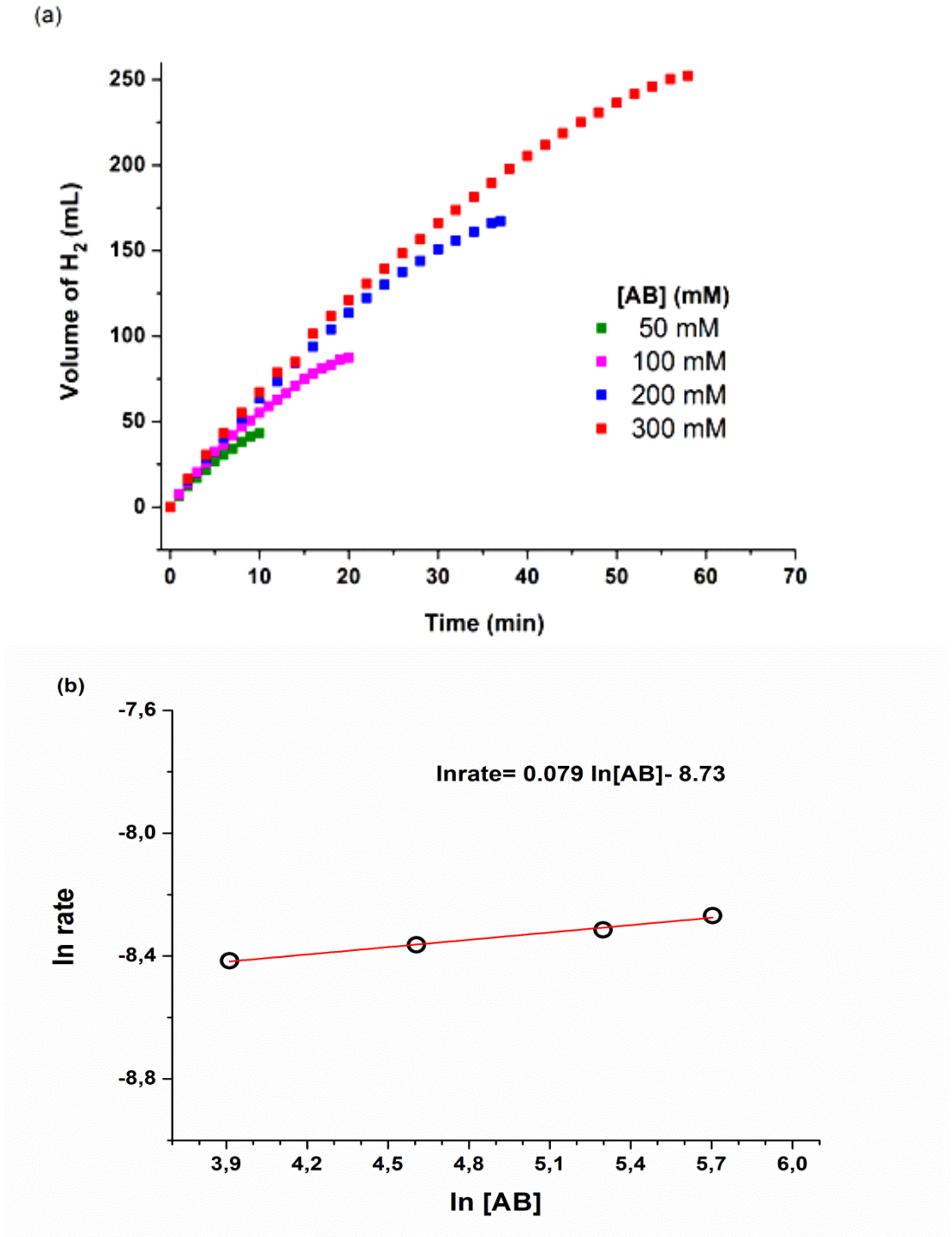

Figure 5.2.3. (a) Plot of mol H_2/mol NH_3BH_3 *versus* time (min) for the hydrolysis of ammonia-borane in various concentrations [NH_3BH_3]=50, 100, 200, 300 mM starting with Rh^{3+}@TiO_2 (with a rhodium content of 0.24% wt) [Rh]=0.1166 mM at 25.0±0.1˚C. **(b)** Plot of the hydrogen-generation rate *versus* the substrate concentration (both in logarithmic scale) in the hydrolysis of NH_3BH_3 catalyzed by *in-situ* generated Rh(0)@TiO_2 at 25.0±0.1˚C.

The next step in kinetic studies, is to find the effect of substrate concentration on the rate of hydrogen generation. For this purpose, various concentrations of ammonia-borane ranging from 50 to 300 Mm were studied at a fixed concentration of 0.1166 mM Rh that is in the form of Rh^{+3}-exchanged titania (anatase) with a rhodium loading of 0.24% wt. at 25.0 ± 0.1˚C (Figure 5.2.3.a).

Figure 5.2.3.b exhibits the plot of hydrogen generation rate *versus* substrate concentrations both in logarithmic scales. The logarithmic graph has the line with the slope of 0.079, indicating that the hydrolysis of ammonia borane is zero-order with respect to the substrate concentration.

The results of the kinetic studies can be used to establish the rate law of the catalytic hydrolysis of ammonia-borane;

$$-\frac{3d\left[NH_3BH_3\right]}{dt} = \frac{d\left[H_2\right]}{dt} = k\left[Rh\right] \qquad (6)$$

In order to find the activation parameters, temperature dependence of the hydrolysis reaction of ammonia-borane catalyzed by *in-situ* generated Rh(0)@TiO_2, was studied at the various temperature in the range of 25-45 °C using the constant concentration of ammonia-borane ([AB]=100 mM) and rhodium ([Rh]=0.116 mM) starting with a Rh^{+3}-exchanged titania. The rate constants for the hydrogen generation at different temperatures were calculated from the slope of linear part of each plot given in Figure 5.2.4.a and used for the calculation of activation energy (Ea=65±2 kJ/mol) from the Arrhenius plot in Figure 5.2.4.b.

The rate constant / temperature data was evaluated according to the Arrhenius equation to obtain the activation energy. The Arrhenius equation was used for the calculating Ea:

$$k=A.e^{-Ea/RT} \quad (7)$$

where A and Ea are constants characteristics of the reaction and R is the gas constant. Ea is the Arrhenius activation energy and A is the pre-exponential factor [73]. Taking the natural logarithm of equation 7, gives equation 8:

$$\ln k = [\ln A-(Ea/RT)] \quad (8)$$

Figure 5.2.4.b shows the Arrhenius plot of lnk versus the reciprocal absolute temperature (1/T). Slope of the straight line gives an activation energy of 65 ± 2 kJ/mol for rhodium(0) nanoclusters catalyzed hydrolysis of ammonia borane. The activation energy for hydrolysis of AB catalyzed by Rh(0)@TiO_2 is comparable to the literature values reported for the same reaction using other catalysts (see Table 1).

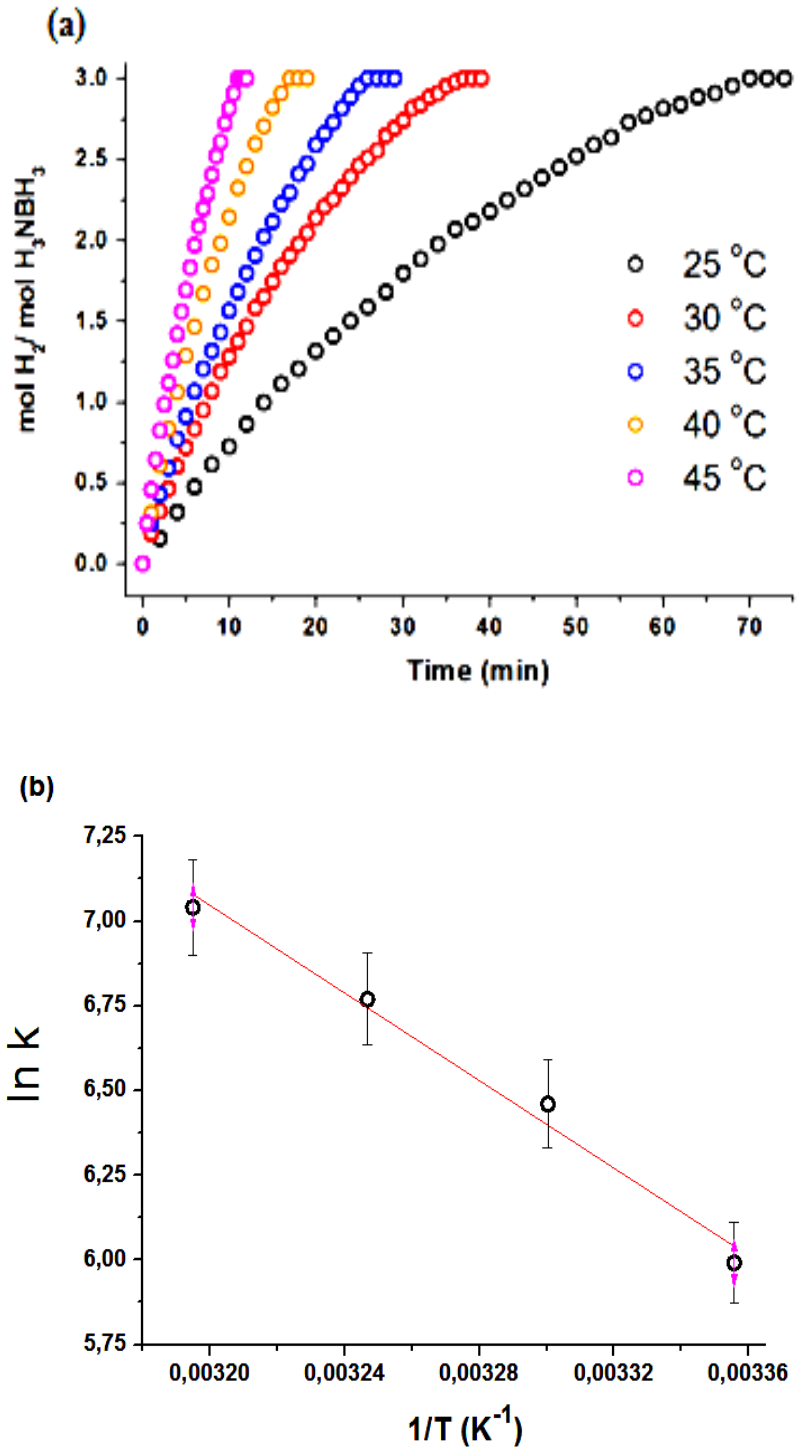

Figure 5.2.4. **(a)** The evolution of equivalent hydrogen per mole of AB versus time plot for the hydrolysis of AB starting with Rh(0)@TiO_2 (0.116 mM Rh) and 100 mM AB at various temperatures, **(b)** The Arrhenius plot for the Rh(0)@TiO_2 catalyzed hydrolysis of AB. *ln*k = -7883.5(1/T) +27.27.

5.3. Catalytic Lifetime and Reusability of Rhodium(0) Nanoparticles Supported on Titania (Anatase) in the Hydrolysis of Ammonia-Borane

Reusability of Rh(0)@TiO_2 catalyst was tested in successive experiments performed using the catalyst isolated from the reaction solution after a previous run of hydrolysis of AB. After the completion of hydrogen generation from the hydrolysis of AB starting with 0.233 mM Rh^{3+}@TiO_2 plus 100 mM AB in 10 mL aqueous solution at 25.0 ± 0.1°C, the catalyst was isolated by centrifugation and washed with 10 mL of water. The isolated sample of Rh(0)@TiO_2 was then redispersed in 10 mL solution containing 100 mM AB and a second run of hydrolysis was started immediately and continued until the completion of hydrogen evolution.

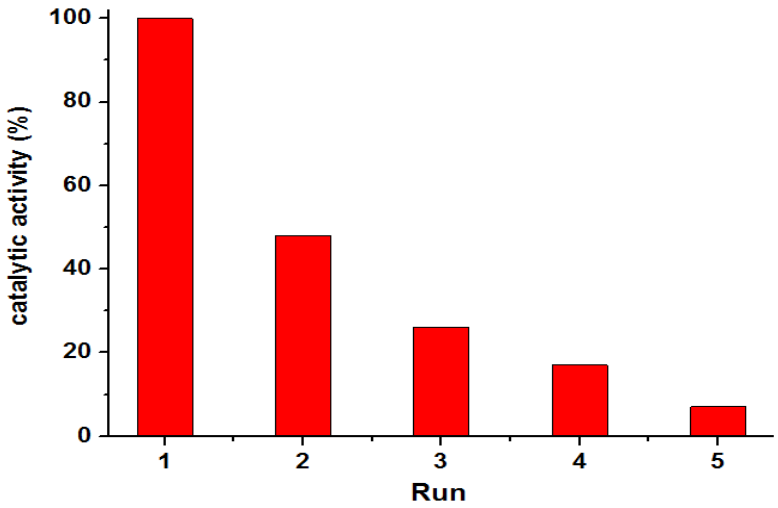

Figure 5.3.1. Percentage of initial catalytic activity of Rh(0)@TiO_2 ([Rh] = 0.233 mM) in successive runs after the reuse for the hydrolysis of ammonia borane (100 mM)

Hydrogen generation process was repeated five times. After the fifth use in hydrolysis of AB, Rh(0)@TiO_2 preserve, it was shown that the catalytic activity of the catalyst decreases to 7.0% of their initial value.

The reusability tests reveal that Rh(0)@TiO_2 are still active in the subsequent runs of hydrolysis of AB providing a release of 3.0 equivalent H_2 per mole of NH_3BH_3.

The catalytic activity of the filtrate solution obtained by centrifugation of the solid materials after the first run of hydrolysis was also tested in the hydrolysis of AB (100 mM) under the same conditions. As shown in Fig. 5.3.2., the filtrate solution shows no catalytic activity in the hydrolysis of AB. This observation supports the conclusion that there is no leaching of rhodium into the solution during the hydrolysis. It also suggests that the rhodium(0) nanoparticles supported on TiO_2 are kinetically competent and heterogeneous catalyst in the hydrolysis of ammonia borane.

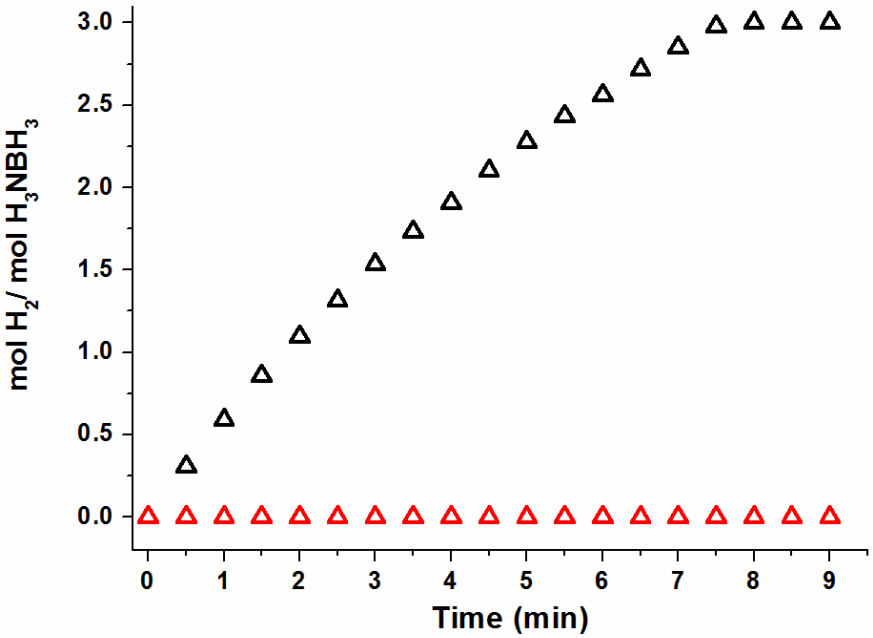

Figure 5.3.2. The evolution of equivalent hydrogen per mole of AB versus time plot for the hydrolysis of AB (100 mM) starting with Rh(0)@TiO_2 (0.233 mM Rh) (Δ), the filtrate solution obtained by centrifugation of the solid materials after the first run, (Δ), at room temperature.

Catalytic lifetime of Rh(0)@TiO_2 was determined by measuring the total turnover number (TTO) in the hydrolysis of ammonia borane. A catalyst lifetime experiment was performed starting with 20 mg Rh^{3+}@TiO_2 (rhodium loading = 0.24% wt. Rh, and [Rh] = 0.0466 mM) in 100 mL solution of AB at 25.0 ± 0.1°C. Figure 5.3.3. shows the variation in turnover number (TON) and turnover frequency (TOF) during the course of the reaction. The TOF value decreases expectedly as the rhodium(0) nanoparticles catalysts are deactivated during the lifetime experiment because of the increasing concentration of metaborate ion.

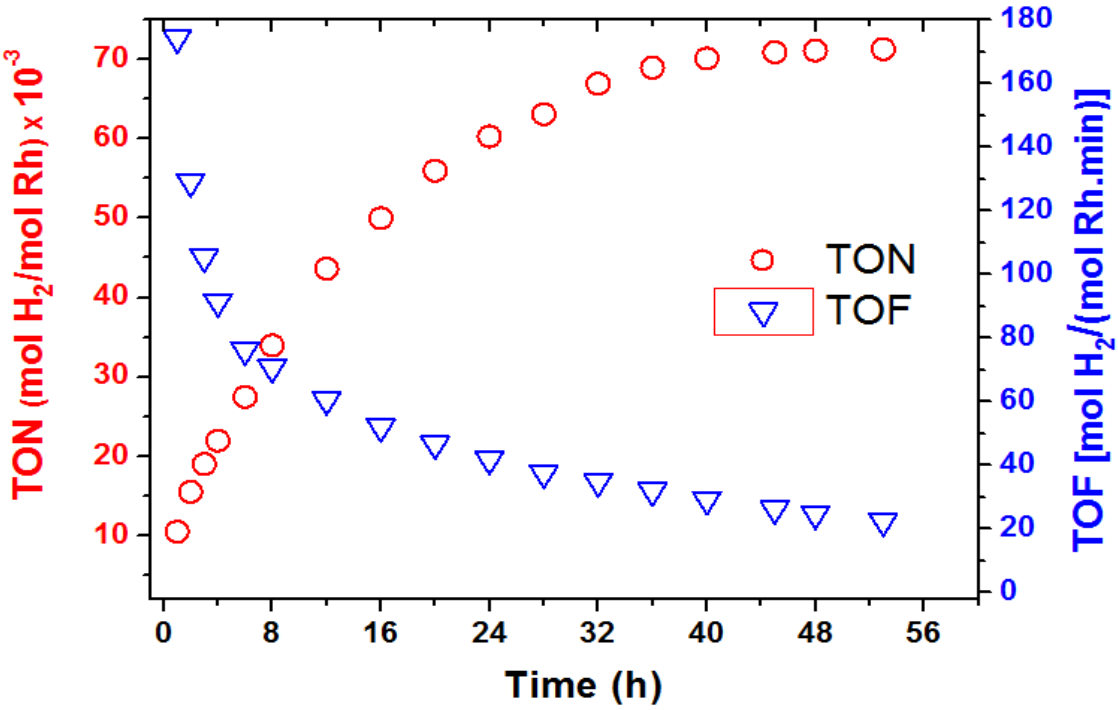

Figure 5.3.3. The variation in turnover number (TON) and turnover frequency (TOF) during the catalytic lifetime experiment performed starting with 20 mg Rh(0)@TiO_2 (rhodium loading = 0.24% wt. Rh, and [Rh] = 0.0466 mM) in 100 mL solution of AB at 25.0 ± 0.1°C.

Rhodium(0) nanoparticles supported on TiO_2 provide 37,350 turnovers over 20 h in the hydrolysis of AB at 25.0 ± 0.1°C before deactivation. As shown in Table

1, TTO value of Rh(0)@TiO_2 for the hydrolysis of ammonia borane is comparable to the literature values reported for the same reaction using other catalysts.

CHAPTER 6

6. CONCLUSIONS

The main findings from this work about preparation and characterization of rhodium(0) nanoparticles supported on titania and their catalytic employment in hydrogen generation from the hydrolysis of ammonia-borane can be summarized as follows:

•Rhodium(0) nanoparticles supported on titania were reproducibly prepared from the reduction of Rh^{3+}@TiO_2 during the catalytic hydrolysis of ammonia borane. Rhodium(III) ions were impregnated on titanium dioxide from the aqueous solution of rhodium(III) chloride and then reduced by ammonia borane at room temperature.

•Highly dispersed rhodium(0) nanoparticles with particle size of the range 1.3- 3.8 nm on titanium dioxide were prepared and characterized by a combination of advanced analytical techniques which are ICP-OES, XRD, SEM-EDS, TEM, XPS and the N_2 adsorption-desorption techniques.

•Rh(0)@ TiO_2 are heterogeneous catalyst and show high catalytic activity in hydrogen generation from the hydrolysis of ammonia borane providing a turnover frequency value up to 260 min^{-1} at 25.0 ± 0.1ºC.

•Rh(0)@TiO_2 are long-lived catalyst providing 37,350 turnovers in hydrogen generation from the hydrolysis of ammonia borane at 25.0 ± 0.1ºC. Rh(0)@TiO_2 are reusable catalyst as they provide the complete hydrolysis of ammonia borane generating 3 mole H_2 per mole of AB even in the fifth use.

•The results of quantitative kinetic study on the hydrogen generation from the hydrolysis of ammonia borane show that the hydrolysis reaction is first order in rhodium concentration and zero order with respect to ammonia borane concentration and the activation energy is 65.5 ± 2 kJ/mol for the hydrogen generation catalyzed by Rh(0)@ TiO_2.

•High catalytic activity and simple preparation procedures make Rh(0)@TiO_2 very attractive catalysts for the hydrolysis of ammonia borane.

REFERENCES

[1] Asif, M., Muneer, T., Renewable and Sustainable Energy Reviews, 2007, 111, 388.

[2] Hansen, J.E., Environmental Research Letters, 2007, 2, 1-6.

[3] http://www.ipcc.ch/pdf/assessment-report/ar4/wg1/ar4-wg1-spm.pdf.

[4] Dell, R.M., Solid State Ionics, 2000, 134, 139-158.

[5] Dillon, A.C., Heben, M.J., Applied Physics A, 2001, 72, 133-142.

[6] Zuttel, A., Naturwissenschaften, 2004, 91, 157–172.

[7] Bockris, J.O.M., International Journal of Hydrogen Energy, 2002, 27,731-740.

[8] Veriroglu, T.N., Barbir, F., International Journal of Hydrogen Energy, 1992, 17, 391.

[9] Licht, S., Chemical Communication, 2005, 4635–4646.

[10] Lee, J.D., Concise Inorganic Chemistry, Wiley-Blackwell, 1999.

[11] Turner, J.A., The Electrochemical Society Interface Fall 2004, 23.

[12] Alfenso, E.Y., Beaird, A.M., Davis, T.,Matthews, M.A., Ind. Eng. Chem. Res., 2009, 48, 3703.

[13] Chen, P., Xiong, Z.T., Luo, J.Z., Lin, J.Y., Tan, K.L., Nature, 2002, 420, 302.

[14] Bacsa, R., Laurent, C., Morishima, R., Suzuki, H., Lelay, M., J Phys Chem B, 2004,108, 12718.

[15] Lim, S.H., Luo, J.Z., Zhong, Z.Y., Ji, W., Lin, J.Y., Inorg. Chem., 2004, 44, 4124.

[16] Dong, J.X., Wang, X.Y., Xu, H,, Zhao, Q., Li, J.P., Int. J. Hydrogen Energy, 2007, 32, 4998.

[17] McKeown, N.B., Budd, P.M., Chem. Soc. Rev., 2006, 35, 675.

[18] Rood, J.A., Noll, B.C., Henderson, K.W., Inorg. Chem., 2006**,** 45, 5521.

[19] Scheideman, M., Wang, G.Q., Vedejs, E.J., Am. Chem. Soc., 2008, 130, 8669.

[20] Sakintuna, B., Lamari-Darkrim, F., Hirscher, M., Int. J. Hydrogen Energy, 2007, 32, 1121.

[21] Umegaki, T., Yan, J-M., Zhang, X-B., Shioyama, H., Kuriyama, N., Xu, Q., Int. J. Hydrogen Energy, 2009, 34, 2303-2311.

[22] (a) Stephens F.H., Pons V., Baker R.T. Dalton Transactions, 2007, 25, 2613; (b) Mohajeri N., Raissi A.T., Adebiyi O., Journal of Power Sources, 2007,167482; (c) Stowe A.C., Shaw W.J., Linehan J.C., Schmid B., Autrey T., Physical Chemistry Chemical Physics, 2007, 9, 1831; (d) Stephens F.H., Baker R.T. MatusM.H., Daniel J., Dixon D.A., Angewandte Chemie International Edition, 2007, 46, 746; (e) Keaton R.J., Blacquiere J.M., Baker R.T., Journal of American Chemical Society, 2007, 129, 1844.

[23] (a) Chandra M., Xu Q., Journal Power Sources 2006, 156, 159; (b) Clark T.J., Whittell G.R., Manners I., Inorganic Chemistry, 2007, 46, 7522; (c) Cheng F.,Ma H., Li Y., Chen J. Inorganic Chemistry, 2007, 46, 788; (d) Chandra M., Xu, Q. Journal Power Sources, 2006, 159, 855; (e) Chandra M., Xu Q., Journal Power Sources, 2006, 163, 364; (f) Chandra M., Xu Q., Journal Power Sources, 2007,168, 135.

[24] Ramachandran V.P., Gagare D.P., Inorganic Chemistry, 2007, 46, 7810.

[25] Wolf, G., Baumann, J., Baitalow, J., Hoffmann, F.P., Thermochim. Acta, 343, 2000, 19- 25.

[26] Yadav, M., Xu, Q., Energy Environ. Sci., 2012, 5, 9698-9725.

[27] Zahmakıran, M., Özkar, S., Nanoscale, 2011, 3, 3462-3481.

[28] Özkar, S., Suib, SL.(Eds.), Batteries, Hydrogen Storage and Fuel Cells, Elsevier, Amsterdam, 2013.

[29] Lu, Z.H., Xu, Q., Func. Mater. Lett., 2012, 5, 1230001-9.

[30] Özkar, S., Finke, R.G., J. Am. Chem. Soc., 2002, 124, 5796-5810.

[31] Özkar, S., Finke, R.G., Langmuir, 2002, 18, 7653-7662.

[32] Varghese, O.K., LaTempa, M.T.J., Grimes, C.A., Nano Lett., 2009, 9, 731-737.

[33] Chen, X., Mao, S.S., Chem.Rev., 2007, 107, 2891-2959.

[34] Reflections on Energy Issues in China, Jiang Ze-min; May 2008; from Journal of Shanghai Jiaotong University.

[35] 'Basic Research Needs to Assure a Secure Energy Future', A Report from the Basic Energy Sciences Advisory Committee (Feb.2003); available at http://www.sc.doe.gov/bes/besac/Basic_Research_Needs_To_Assure_A_Secure_Energy_Future_FEB2003.pdf.

[36] The General Characteristic of World Energy Situation; January 2007; from www.in-en.com.

[37] Penner S.S., Energy, 2006, 31, 33-43.

[38] U.S Energy of Administration, Annual Energy Review, 2011, http://www.eia.gov/totalenergy/data/annual/pdf/aer.pdf.

[39] United State Department of Energy. (2004). Hydrogen Posture Plan: An Integrated Research, Development and Demonstration Plan. Strategic Plan.

[40] Scott DS. Smelling land, the hydrogen defence against climate catastrophe. Montreal: Price-Patterson, http://www.H2.ca, 2006.

[41] United States Department of Energy, 'National Hydrogen Energy Roadmap, ' (Washington DC:US DOE, 2002), p.iii.

[42] Ibid., pp. 17-22.

[43] Ibid., pp. 13-16.

[44] Amos, W.A. (1998). Costs of Storing and Transporting Hydrogen. Technical Report, National Renewable Energy Laboratory.

[45] Nexant, Inc.; Air Liquide; Argonne National Laboratory; Chevron Technology Venture; Gas Technology Institute; National Renewable Energy Laboratory; Pacific Northwest National Laboratory; Tiax LLC. (2008). H2A Hydrogen Delivery Infrastructure Analysis Models and Conventional Pathway Options Analysis Results. Interim Report.

[46] Nowotny, J., Bak, T., Chu, D., Fiechter, S., Murch, G., Veziroğlu, T., International Journal of Hydrogen Energy, 2014, 39, 4151-4157.

[47] Schlapbach, L., Zuttel, A., Nature, 2001, 414, 353.

[48] Grochala, W., Edwards, P.P., Chem. Rev. 2004, 104, 1283.

[49] Orimo, S., Nakamori, Y., Eliseo, J.R., Zuettel, A., Jensen, C.M., Chem. Rev. 2007, 107, 4111.

[50] Seayad, A.M., Antonelli, D.M., Adv. Matter, 2004, 16, 765.

[51] Richardson, B.S., Birdwell, J.F., Pin, F.G., Jansen, J.F., Lind, R.F., J.Power Sources, 2005, 145, 21.

[52] a) Sandrock, G., Reilly, J., Graetz, J., Zhou, W.H., Johnson, J., Wegrzyn, J., Appl.Phys. A 2005, 80, 687. b) Graetz, j., Reilly, J.J., Phys.Chem.B 2005,109,22181.

[53] (a) Amendola S.C., Janjua J.M., Spencer N.C., Kelly M.T., Petillo P.J., Sharp Goldman S.L., Binder M., Int. J. Hydrogen Energy, 2000, 25, 969-975. (b) Lee J.Y., Lee H.H., Lee J. H., Kim D.M., Kim J.H., J. Electrochem. Soc., 2002, 149, 603-606.

[54] Mohajeri, N., Adebiyi, O., Baik, J., Bokerman, G., Raissi, A.T., Prepr.Symp, -Am. Chem.Soc.Div.Fuel Chem., 2006,51,520.

[55] Bluhm, M.E., Bradley, M.G., Butterick, R., Kusari, U., Sneddon, L.G., J.Am.Chem.Soc., 2006,128,7748.

[56] Denney, M.C., Pons, V., Hedben, T.J., Heinekey, D.M., Goldberg, K.I., J.Am.Chem.Soc., 2006,128,12048.

[57] a) Hu, M.G., Geanangel, R.A., Wendlandt, W.W., Thermochim.Acta 1978,23,249. b) Sit, V., Geanangel, R.A., Wendlandt, W.W., Thermochim.Acta 1987,113,379.

[58] a) Baitalow, F., Baumann, J., Wolf, G., Jaenicke-Röbler, K., Leitner, G., Thermochim. Acta, 2002, 391, 159. b) Baumann, J., Baitalow, F., Wolf, G., Thermochim. Acta, 2005,430,9.

[59] a) Gutowska, A., Li, L.Y., Shin, Y.S., Wang, C.M.M., Li, X.H.S., Linehan, J.C., Smith, R.S., Kay, B.D., Schmid, B., Shaw, W., Gutowski, M., Autrey, T., Angew.Chem.Int.Ed., 2005, 44, 3578. b) Feaver, A., Sapehri, S., Shamberger, P., Stowe, A., Autrey, T., Cao, G.Z., J.Phys.Chem.B, 2007,11,7469.

[60] Kalidindi, S.B., Sayal, U., Jagirdar, B.R., Phys.Chem.Chem.Phys., 2008, 10, 5870-5874.

[61] Basu, S., Brockman, A., Gagore, P., Zheng, Y., Ramachandran, P.V., Delgass, W.N., Gore, J.P., J. Power Sources, 2009, 188, 238-243.

[62] Yan, J. -M., Zhang, X. -B., Han, S., Shioyama, H., Xu, Q., J.Power Sources, 2009, 194, 478-481.

[63] Yan, J-M., Zhang, X-B., Han, S., Shioyama, H., Xu, Q., J.Power Sources, 2010, 195, 1091-1094.

[64] Kelly, H.C., Marriott, V.B., Inorg.Chem., 1979, 18, 2875.

[65] Ryschkewitsch, G.E., J.Am.Chem.Soc., 1960, 82, 3290-3294.

[66] Zahmakıran, M., Özkar, S., Appl.Catal.B: Env., 2009, 89, 104-110.

[67] Durap, F., Zahmakıran, M., Özkar, S., Int.J.Hydrogen Energy, 2009, 34, 7223-7230.

[68] Aiken III J.D., Lin Y., Finke R.G., J. Mol. Catal. A., 1996, 114, 29-51.

[69] Schmid G. (Ed), Clusters and Colloids: From Theory to Applications, VCH Publishers, New York, 1994

[70] Jongh L.J.(Ed), Physics and Chemistry of Metal Cluster Compounds, Kluwer Publishers, Dordrect, 1994.

[71] Simon, U., Schön, G., Schmid, G., Angew Chem. Int. Ed. Eng., 1990, 248, 1186.

[72] Glanz, J., Science, 1995, 269, 1363.

[73] Schon, G., Simon U., Colloid Polym. Sci., 1995, 273, 202.

[74] Antonietti, M., Göltner, C., Angew. Chem., Int. Ed. Eng., 1997, 36 910–928.

[75] Elghanian, R., Storhoff, J.J., Mucic, R.C., Setinger, R.L., Mirkin, C.A., Science, 1997, 277, 1078.

[76] Colvin, V.L., Schlamp, M.C., Alivisatos, A.P., Nature, 1994, 370, 354.

[77] Sonti, S.V., Bose, A., J. Colloid Int. Sci., 1995, 170, 575.

[78] M.T. Reetz, M. Winter, G. Dumpich, J. Lohau, S. Friedrichowski, J. Am. Chem. Soc. 119 _1997. 4539–4540.

[79] T. Vossmeyer, E. DeIonno, J.R. Heath, Angew. Chem., Int. Ed. Engl. 36 _1997. 1080.

[80] (a)Schmid, G., Maihack, V., Lantermann, F., Pechel, S., J. Chem. Soc. Dalton Trans., 1996, 199, 589 (b) Lin, Y., Finke, R. G., J. Am. Chem. Soc., 1994, 116, 8335. (c) Bönneman, H.; Braun, G.A., Angew Chem. Int. Ed. Eng., 1996, 35, 1992. (d) Lewis, L.N.; Lewis, N., J. Am. Chem. Soc., 1986, 108, 7228. (e) Wilcoxon, J.P.; Martinho, T.; Klavetter, E.; Sylwester, A.P., Nanophase Mater. 1994, 771. (f) Na, Y.; Park, S.; Bong, S.H.; J. Am. Chem. Soc., 2004, 126, 250. (g) Pelzer, K.; Vidoni, O.; Phillot, K.; Chaudret, B.; Colliére, V., Adv. Func. Mater., 2003, 12, 118. (h) Hostetler, M.; Wingate, J.; Zong, C.; Evans, N.; Murray, R., Langmuir, 1998, 14, 17-30 (ı) Pelzer, K.; Phillot, K.; Chaudret, B., Z. Anorg. Allg. Chem., 2003, 629, 1217.

[81] Pool R., Science, 1990, 248, 1186-1188.

[82] Schmid, G., Endeavour, 1990, 14, 172.

[83] Wu, B., Zheng, N., Nano Today, 2013, 8, 168-197.

[84] Morup, S., Hansen, M.F., Frandsen, C. (Eds.), Elsevier; 2011, 153-201.

[85] Kalele, S., et-al. Current Science, 2006, 91(8), 1038-1052.

[86] Nilius, N., Wallis, T.M., Ho, W., Science, 2002, 297, 1853-1856.

[87] Guczi, L., Paszti, Z., Peto, G., Corain, B., Schmid, G., Toshima, N. Amsterdam: Elsevier; 2008, 77.

[88] Rao, C.N.R., Thomas, P.J., Kulkarni, G.U.(Eds.), NW: Springer, 2007,95.

[89] Finke R. G. In *Metal Nanoparticles: Synthesis, Characterization and Applications*; Feldheim, D. L., Foss, C. A., Jr., Eds.; Marcel Dekker: New York, 2002; Chapter 2, pp 17-54.

[90] Aiken, J.D., III; Finke, R.G.J. Mol. Catal. A: Chem. 1999, 145, 1.

[91] Hirtzel, C.S., Rajagopalan, R. In Colloidal Phenomena: Advanced Topics; Noyes: New Jersey, 1985; 27-39 and 73-87.

[92] Goodwin, J.W., The Royal Society of Chemistry: London, 1982.

[93] Hiemenz, P.C. In Principles of Colloid and Surface Chemistry, Marcel Dekker: New York, 1986.

[94] Hunter, R.J. In Foundations of Colloid Science; Oxford University Press: New York, 1987, 1, 316.

[95] Ross, S., Morrison, I.D. In Colloidal Systems and Interfaces, Wiley: New York, 1988.

[96] Everett, D.H., Royal Society of Chemsitry: London, 1988.

[97] Evans, D.F. Wennerstrom, H. In The Colloidal Domain, 2nd ed., Wiley-VCH: New York, 1999.

[98] Labib, M.E. Colloids Surf., 1988, 29, 293.

[99] Napper, D.H. In Polymeric Stabilization of Colloidal Dispersions, Academic Press: London, 1983.

[100] Lin, Y., Finke, R.G.J. Am. Chem. Soc., 1994, *116*, 8335.

[101] Bönneman, H., Richards, R. M., Eur. J. Inorg. Chem., 2001, 10, 2445.

[102] (a) Reetz, M.T., Helbig, W., Quaiser, S.A., In Active Metals:Preparation, Characterization, Applications, VCH: New York, 1996. (b) Reetz, M. T., Helbig, W., J. Am. Chem. Soc., 1994, 116, 7401.

[103] (a) Tano, T., Esumi, K., Meguro K.J. Colloid Interface Sci., 1989, 133, 530. (b) Esumi, K., Tano, T., Meguro, K., Langmuir, 1989, 5, 268. (c) Dhas, N. A., Suslick, K. S., J. Am. Chem. Soc., 2005, 127, 2368. (d) Suslick, K A., Choe, S.-B., Cichowias, A. A., Grinstaff, M. W., Nature, 1991, 353, 414.

[104] Takahashi Y., Ito T., Sakai S., Ishii Y., Chem. Commun., 1970, 1065.

[105] Klabunde, K.J., Habdas, J., Cardenas-Trivino, G., Chem. Mater., 1989, 1, 481.

[106] Iwasawa Y., Tailored Metal Catalysts, Kluwer, Dordrecht, 1986.

[107] Williams, D.B., Carter, C.B., Transmission Electron Microscopy, A Textbook for Materials Science, Plenum, New York, 1996.

[108] Thomas J.M., Thomas W.J., VCH Publishers Inc; New York, 1999.

[109] Shriver D.F., Atkins P.W., Inorganic Chemistry, Oxford University Press, 1999.

[110] Smith, G.V., Notheisz, F., Heterogeneous Catalysis in Organic Chemistry; Academic Press, San Diego**,** 1999.

[111] Zaera, F., Surface Science, 2002, 500, 947-965.

[112] Blaser, H.U. Catalysis Today, 2000, 60, 161-165.

[113] Gates, B.C., "Catalytic Chemistry", John Wiley & Sons, 1992.

[114] Baer, Y., Heden, P.F., Hedman, J., Klasson, M., Nordling, C., Siegbahn, K., Phys. Scripta, 1970, 1, 55-65.

[115] Mevellec, V., Nowicki, A., Roucoux, A., Dujardin, C., Granger, P., Payen, E., Philippot, K., New J. Chem., 2006, 30, 1214-1219.

[116] Akbayrak, S., Özkar, S., ACS Appl. Mater. Interfaces, 2012, 4, 6302-6310.

[117] Akbayrak, S., Gençtürk, S., Morkan, İ., Özkar, S. RSC Advances, 2014, 4, 13742-13748.

[118] Durap, F., Zahmakıran, M., Özkar, S., Appl. Catal. A: General, 2009, 369, 53-59.

[119] Metin, Ö., Sahin, S., Özkar, S., Int. J. Hydrogen Energy, 2009, 34, 6304-6313.

[120] Akbayrak, S., Erdek, P., Özkar, S., Appl. Catal. B: Environ., 2013, 142-143, 187-195.

[121] Chen, GZ., Desinan, S., Nechache, R., Rose, R., Rose, F., Ma, DL., Chem. Commun., 2011, 47**,** 6308-6310.

[122] Cao, N., Luo, W., Cheng, G., Int. J. Hydrogen Energy, 2013, 38, 11964-72.

[123] Zahmakıran, M., Mater. Sci. Eng. B, 2012, 177, 606-613.

[124] Wang, J., Qin, Y-L., Liu, X., Zhang, X-B. J. Mater. Chem., 2012, 22, 12468-12470.

[125] Sun, D., Mazumder, V., Metin, Ö., Sun, S. ACS Nano, 2011, 5, 6458-6464.

[126] Kılıç, B., Sencanlı, S., Metin, Ö. J. Molecular Catal. A: Chemical, 85 2012, 361-362, 104-110.